# NEURO- AND GLIOGENESIS IN THE PUBERTAL RAT BRAIN: IMPLICATIONS FOR FEMALE REPRODUCTION

By

Margaret Ann Mohr

A DISSERTATION

Submitted to
Michigan State University
in partial fulfillment of the requirements
for the degree of

Neuroscience – Doctor of Philosophy

2015

**ABSTRACT**

NEURO- AND GLIOGENESIS IN THE PUBERTAL RAT BRAIN: IMPLICATIONS IN FEMALE REPRODUCTION

By

Margaret Ann Mohr

Puberty and adolescence are associated with a gain of function in brain circuits that regulate sex-specific physiology and behavior. One of the most striking sex differences to arise during puberty in rats is the capacity to generate a surge of luteinizing hormone (LH), which females, but not males, produce as part of ovarian cyclicity. The preovulatory LH surge is controlled by the anteroventral periventricular nucleus of the hypothalamus (AVPV). The AVPV is sexually dimorphic in structure; in females the AVPV is larger and contains more neurons compared to males. Previous work in my advisor and co-advisor's laboratory has demonstrated sex differences in the addition of new cells, including both neurons and glia, to the AVPV during puberty. Gonadal hormones drive these particular sex differences, as they are abolished by prepubertal gonadectomy. A key question is whether these newly added cells contribute to the sex-specific regulation of physiology and behavior that arises during puberty. Because the LH surge cannot be elicited before puberty in female rats, perhaps the cellular machinery responsible for regulation of the LH surge and ovarian cyclicity is not yet in place. The goal of the experiments conducted in this dissertation was to test the hypothesis that ***cells added to the AVPV during puberty are functionally incorporated into the neural circuitry involved in female-specific regulation of the hypothalamic- pituitary-gonadal (HPG) axis that controls the LH surge and ovarian cyclicity***. The first aim replicated a sex difference previously seen in the addition of cells to the AVPV during puberty and determined that this sex difference was due to

greater cell addition in female rats compared to males. Furthermore, it employed immunofluorescent labeling to determine that pubertally born cells in the AVPV include neurons, astrocytes, and microglia. The second aim determined that pubertally and adult-born cells are active at the time of the LH surge, and that knockdown of either pubertally or adult-born cells attenuated and delayed the LH surge. These studies further our understanding of the function of pubertally added cells to sexually dimorphic brain regions, and have provided insight into how sex- specific regulation of the HPG axis is established during puberty and maintained in adulthood.

Dedicated in loving memory to LBM.

ACKNOWLEDGEMENTS

None of this work could have been done if it were not for the collaborative environment of the Sisk laboratory. Jane Venier, Rayson Figueira, Dr. Margaret Bell, and Dr. Kayla De Lorme taught me everything that I needed to know about how to work with BrdU and the procedures that are widely used throughout my dissertation. Ray helped me get the AraC project off the ground and provided invaluable technical assistance throughout the time we overlapped. Andrew Kneynsberg also played a large role in AraC pilot experiments and optimization of double- and triple-label immunofluorescent protocols. Dr. Nancy Michael played an instrumental part in some of the studies in chapter 1. Elaine Sinclair helped with almost every surgery in this dissertation, and whose company has been irreplaceable. Jenny Kim also helped with most surgeries and has provided valuable input throughout the way, while keeping a smile on my face. Finally, I am immeasurably grateful to Jane Venier, for helping me every step of the way, particularly in regards to blood sampling and the LH RIAs. Her advice and support has been instrumental in my success.

I am also hugely thankful to my advisor and collaborator, Dr. Lydia DonCarlos, whose continued support has contributed to my success. I have been privileged to work with such an amazing neuro-anatomist and scientist. I owe a huge bit of thanks to her technician, Francisca Garcia, with whom I have worked on the BrdU projects from the very beginning. Fran played a vital role in most the experiments from Chapter 1.

Finally, I extend a heartfelt appreciation to my advisor, Dr. Cheryl Sisk, who has supported and trusted in me all along the way. She taught me critical thinking skills, patience, and has been a true role model of a scientist, writer, and great person in general.

**TABLE OF CONTENTS**

## LIST OF TABLES

## LIST OF FIGURES

## KEY TO ABBREVIATIONS

| | |
|---|---|
| analysis of variance | ANOVA |
| cytosine arabinofuranoside | AraC |
| anteroventral periventricular nucleus of the hypothalamus | AVPV |
| 5-bromo-2'-deoxyuridine | BrdU |
| dentate gyrus | DG |
| estrogen/estradiol | E |
| estradiol | E2 |
| estradiol benzoate | EB |
| epidermal growth factor | EGF |
| estrogen receptor alpha | ERα |
| glial fibrillary acidic protein | GFAP |
| gonadotropin-releasing hormone | GnRH |
| hypothalamic-pituitary-gonadal | HPG |
| Ionized calcium binding adaptor molecule 1 | Iba1 |
| intracerebroventricular | ICV |
| immediate early gene | IEG |
| insulin-like growth factor-1 | IGF-1 |
| intraperitoneal | ip |
| luteinizing hormone | LH |
| membrane estrogen receptor alpha | mERα |
| medial preoptic area | MPOA |

| | |
|---|---|
| neuronal nuclei | NeuN |
| neurally synthesized progesterone | neuroP |
| ovariectomized | OVX |
| progesterone | P |
| postnatal day () | P() |
| proliferating nuclear cell antigen | PCNA |
| preoptic area | POA |
| progesterone receptor | PR |
| radioimmunoassay | RIA |
| sexually dimorphic nucleus of the preoptic area | SDN-POA |
| standard error of the mean | SEM |
| subgranular zone | SGZ |
| subventricular zone | SVZ |
| Tris-buffered saline | TBS |
| testosterone propionate | TP |
| ventromedial hypothalamus | VMH |

## INTRODUCTION

The physiological and behavioral events surrounding puberty are shrouded in mystery. Puberty is characterized by the awakening of the hypothalamic-pituitary-gonadal (HPG) axis and results in sexual maturation. Rodents provide an excellent model with which to study the fundamental processes that govern puberty. While great steps have been made to determine the cellular mechanisms underlying the pubertal transformation, many questions remain unanswered. One question of particular interest is: how does the brain change during puberty to enable a female, but not a male rodent, to begin to exhibit estrogen positive feedback that allows for regular estrous cyclicity?

### *The AVPV as the conductor of the preovulatory GnRH and LH surge*

The AVPV is a necessary element of the female HPG axis, as it plays a crucial role in estrogen positive feedback to allow for both the onset of puberty and the induction of the luteinizing hormone (LH) surge. Estradiol acts within the AVPV to induce GnRH release that causes the surge in LH (reviewed in (Simerly, 2002)). Although the first studies implicating the AVPV as the site of estrogen-positive feedback in the rat did not investigate the AVPV directly, these studies paved the way for thinking about the AVPV as a crucial component of the positive feedback effects of estradiol on the LH surge. In the 1970s, two separate groups found that 17β estradiol placed into the medial preoptic nucleus elicited an LH surge (Goodman, 1978; Kalra and McCann, 1975). A decade later Sandra Petersen demonstrated that delivery of anti-estrogens into this same area blocked the estrogen-induced surge in LH, and also affected gonadotropin-releasing hormone (GnRH) mRNA (Petersen and Barraclough, 1989; Petersen et al., 1989).

Several lesion studies have implicated the AVPV, but not nearby areas, in the estrogen- or estrogen plus progesterone-induced LH surge. Small electrolytic lesions to the AVPV in normally cycling adult female rats induced persistent vaginal cornification, indicative of persistent estrus (Wiegand et al., 1980). Furthermore, when the same small electrolytic lesions were made to the AVPV, persistent estrus was observed in animals treated with estradiol benzoate followed by progesterone, indicating that the AVPV is a crucial component of the estrogen and progesterone positive-feedback effects on GnRH release (Wiegand and Terasawa, 1982).

***Development of estrogen-positive feedback in the female rat***

Estrogen-positive feedback in the female rat occurs throughout the juvenile time period. During the infantile period, sufficiently high doses of estrogen actually *suppress* circulating levels of LH, indicating that the estrogen-negative feedback mechanism is in place early in life (Ojeda SR, 1994). However, a stimulatory effect of estradiol on LH release is not observed until postnatal day (P)16, where from P16-P20 the amount of estradiol required to elicit a surge in LH is twice as high as levels of E that are observed on proestrus. Starting around P22, the LH surge can be induced with proestrus-levels of estradiol, however the timing of the surge is different than in mature animals, as it takes about 54 h after administration of estradiol. By P30, the LH surge can occur within 30 hrs with an amplitude that is indistinguishable from proestrus animals (Andrews et al., 1981). Thus, to understand how estrogen positive feedback emerges during puberty, we must first understand how the AVPV is structurally remodeled during puberty.

***Morphological sex differences of the AVPV: when do they emerge?***

The AVPV is an uncommon brain structure in that it is female biased, i.e., larger and contains more cells in females compared to males, whereas many sexually dimorphic brain structures such as the medial amygdala, the sexually dimorphic nucleus of the preoptic area (SDN-POA), and bed nucleus of the stria terminalis are male biased. In 1982, Bleier and colleagues documented a female biased sex difference in cell distribution and density in what would later be named the AVPV in young adult rats, guinea pigs, hamsters, and mice (Bleier et al., 1982). In adulthood, the AVPV is roughly 1.6 times larger in females compared to males (Bloch and Gorski, 1988). In the next few years, investigators found that treating neonatal or perinatal females with testosterone eliminated the sex difference in AVPV volume in adulthood, and that testosterone was acting to increase cell death (Ito et al., 1986; Nishizuka et al., 1993; Sumida et al., 1993).

These results are consistent with the idea that gonadal hormones act during the critical perinatal period to induce sexual differentiation of brain structures. However, while gonadal hormones during the perinatal period seem important for sexual differentiation of the AVPV, a peculiar finding by Davis, Shryne, and Gorski in 1996 pointed to the *pubertal* period as the period when the sex difference in AVPV volume becomes morphologically detectable. In this study, they found that the sex difference in AVPV volume develops between P30-40 and that the sex difference in AVPV length develops between P60-80. Castrating a male rat on the day of birth increases AVPV volume to that of a female AVPV while ovariectomy of a female rat on the day of birth has no later effect on AVPV volume (Davis et al., 1996). Cell addition to the AVPV was not considered as a feasible mechanism to cause these volumetric differences, because at

the time, neurogenesis was only thought to occur in discrete regions of the brain. Thus, it was concluded that perinatal androgens drive cell death in the male AVPV. The authors attributed the volumetric differences that arose after puberty to be the result of increased diameter of neurons and glia, or changes in the nature or density of synaptic contacts within the AVPV.

Of the processes that could maintain sexual dimorphisms in AVPV volume, cell death must not be overlooked. In a series of elegant studies by the laboratory of Dr. Nancy Forger and colleagues, cell death was determined to be the cellular mechanism that drove the morphological sex differences in the AVPV. Both over-expression of Bcl-2 (an anti-apoptotic protein) and knockout of Bax (a protein critical to cell death) eliminate the sex difference in cell number and volume in the mouse AVPV where over-expression of Bcl-2 caused an increase in AVPV cell density in males to that of wildtype females, but had no effect in females (Zup et al., 2003) and Bax knockout increased AVPV cell number in both sexes, but there was no sex difference in cell number between transgenics (Forger et al., 2004).However in both cases, a highly sexually dimorphic population of dopaminergic cells within the AVPV (Simerly et al., 1985) is unaffected by these genetic manipulations. This dopaminergic population of cells in the AVPV and conceivably others as well acquire sexual dimorphisms through processes that are independent of cell death, such as hormonally programmed cell addition.

***The addition of cells to the AVPV during puberty***

Because the effects of perinatal gonadal hormones on gross morphology of the AVPV are not apparent until after puberty, when gonadal hormone secretion rises, and cell death does not affect every cell population within the AVPV, it makes sense to consider that gonadal hormones might be promoting the addition of new cells to the AVPV during puberty. Indeed, a

study published by the DonCarlos and Sisk laboratories showed that there are sex differences in the addition of cells to sexually dimorphic brain regions and that gonadal hormones drive these sex differences (Ahmed et al., 2008). Specifically, more cells are added to the female rat AVPV during puberty compared to the male. Prepubertal gonadectomy banishes the sex difference in addition of cells to the AVPV. The opposite pattern is true in the medial amygdala and the SDN-POA, where males have more cells added to these male-biased brain regions during puberty compared to females. These data point to hormonally mediated cell addition as a mechanism to actively maintain morphological sex differences throughout puberty, and possibly adulthood. One tantalizing idea is that this cell addition during puberty also contributes to physiological and behavioral sex differences. In other words, does hormonally mediated cell addition during puberty contribute to sex-specific gain of function that arises during puberty?

***The functional significance of pubertally born cells: using the AVPV and the LH surge as a model***

To begin to understand the functional significance of pubertally born cells, we determined that pubertally born cells were active during mating in adult male hamsters (Mohr and Sisk, 2013). Male hamsters were given cell proliferation marker 5-bromo-2'-deoxyuridine (BrdU) every day during puberty (P28-P49). In adulthood, the P77 males were paired with a sexually receptive female and allowed to mate. The male hamsters were perfused an hour after the mating experience, which is sufficient time for the expression of Fos, the protein product of immediate early gene *c-fos* and indicator of cellular activation. BrdU and Fos immunoreactivity indicated that some pubertally born cells were active during mating in all regions analyzed (dentate gyrus of the hippocampus, the medial preoptic area and the arcuate nucleus of the

hypothalamus, and the subdivisions of the medial amygdala). Furthermore, some of the pubertally born cells in these regions were determined to be neurons or astrocytes. The results of this study led us to the conclusion that pubertally born cells become functionally incorporated into neural circuits involved in sociosexual behavior in adulthood. However, mating is a complex behavior that relies on interactions between two individuals, and many factors can affect these interactions. Therefore, mating might not be the best model to test if cell addition contributes to functional sex differences that arise during puberty. In other words, it would be better to use a simpler sex-specific model system, such as generation of the LH surge, which does not rely on interactions with another individual.

Much like mating in rodents, the LH surge cannot occur until after puberty. Only after 28 days of age will a female rat elicit a temporally relevant LH surge in response to preovulatory levels of estradiol (i.e., before 28 days of age a rat will display a LH surge that is delayed or that requires supra-physiological levels of estradiol) (Andrews et al., 1981). Moreover, male rats given E and P are unable to elicit a LH surge, regardless of age (Hoffman et al., 2005). These aforementioned characteristics of the LH surge make it a precise model to test whether cells added to the female rat AVPV during puberty contribute to *sex-specific* gain of function that occurs during this transformative time.

***Concluding remarks***

The objective of this dissertation is to test the hypothesis that pubertally born cells are functionally incorporated into neural circuits that are important for sex-specific regulation of the HPG axis. A number of experiments were conducted to answer different aspects of this hypothesis. First, I confirmed the sex difference in the addition of pubertally born cells to the

AVPV and then asked whether these cells differentiated into neurons, astrocytes, or microglia. Then, I determined if cells that are added to the AVPV during puberty are active during the LH surge. Finally, I determined if cells added to the brain during or after puberty are necessary for the ability to generate a LH surge.

***Summary of Dissertation Experiments***

**Chapter 1:** I will first determine if the sex difference in the number of pubertally born cells in the rat AVPV is due to greater cell proliferation, survival, or both in females compared to males, by giving BrdU to female and male rats on postnatal day (P) 30 and perfusing the animals at short (to evaluate cellular proliferation) and longer (to evaluate cell survival) time intervals following BrdU treatment. Then I will validate that cell proliferation is occurring within the AVPV and confirm the use of BrdU as a birthdating marker by giving female rats BrdU on P30 and perfusing them from very short (2 h) to longer (21 d) timepoints to look at BrdU and proliferating nuclear cell antigen (PCNA) colocalization. Finally, I will determine if cells added to the female rat AVPV during puberty are neurons, astrocytes, or microglia by giving BrdU to female rats every day during puberty and perfusing them on P77 to look at BrdU colocalization with neuronal nuclei (NeuN), glial fibrillary acidic protein (GFAP), or ionized calcium binding adaptor molecule 1 (Iba1).

**Chapter 2:** First I will determine when, in our hands, the LH surge (and AVPV Fos expression corresponding to the surge) occurs after hormone priming. I will then determine if pubertally born cells in the female rat AVPV are active during the LH surge by giving central BrdU throughout puberty (to maximize BrdU labeling), perfusing the animals during a hormone-elicited LH surge in adulthood, and looking at BrdU and Fos colocalization. I will also perform

BrdU labeling with estrogen receptor alpha (ERα) and progesterone receptor (PR) to determine if newly born cells share phenotypic characteristics of known regulators of estrogen positive feedback. Finally, I will determine if cell addition to the brain during or after puberty is necessary for the ability to generate a LH surge by administering mitotic inhibitor cytosine β-d arabinofuranoside (AraC) during or after puberty and testing for the ability to elicit a LH surge. This final experiment will also determine if cell addition occurs in the AVPV during adulthood, and whether cell addition in the AVPV is a life-long mechanism to support sex-specific regulation of the HPG axis.

## CHAPTER 1

Neuro- and Gliogenesis in the Female Rat Brain During Puberty

## INTRODUCTION

The onset of puberty, and consequently the upswing of gonadal hormone secretion, initiates extensive remodeling of several brain regions. One such region is the anteroventral periventricular nucleus (AVPV) of the hypothalamus, the brain region responsible for estrogen positive feedback and generation of the preovulatory surge in luteinizing hormone (LH), an event critical to reproduction (for review see (Simerly, 2002)).

The AVPV is sexually dimorphic in morphology, where it is larger and contains more neurons in females compared to males (Davis et al., 1996), as well as functionally, where it controls the LH surge in female, but not male rodents (Hoffman et al., 2005). Only after puberty are these structural and functional sexual dimorphisms observable; the morphological sex difference becomes apparent only after puberty (Davis et al., 1996) and only after puberty can females mount a LH surge that is temporally and physiological relevant (Andrews et al., 1981), thus highlighting the importance AVPV remodeling during the pubertal time period.

Previous studies from our laboratory have demonstrated a hormonally mediated addition of cells to sexually dimorphic brain regions during puberty, including the AVPV, where pubertal female rats have more cells added to the AVPV compared to pubertal male rats. Removal of ovarian hormones prior to puberty eliminates this sex difference (Ahmed et al., 2008).

To determine whether this sex difference in the number of pubertally born cells in the AVPV of young adult rats is due to sex differences in cell addition, cell survival, or both, three

injections of cell proliferation marker bromodeoxyuridine (BrdU) were given to male and female rats on a single day in early puberty, postnatal day (P) 30, and animals were perfused at five time points, from 2 to 42 days after BrdU. Earlier time points helped determine if there were sex differences in cell proliferation, while later time points helped determine if there were sex differences in the survival of cells born during early puberty in the AVPV. Next, to determine whether cell proliferation was indeed occurring in the AVPV, BrdU was given once to female rats on P30 and were perfused at 9 timepoints, from 2 hours to 21 days, after BrdU treatment. Immunofluorescent labeling of BrdU with the proliferation marker, proliferating nuclear cell antigen (PCNA) was performed. Finally, to determine if cells that are born during puberty in the female rat AVPV are neurons, astrocytes, or microglia, females were given BrdU daily for 4 weeks during puberty (P28-56), perfused on P77, then immunofluorescent labeling of BrdU with mature neuronal nuclei marker (NeuN), astrocyte marker glial fibrillary acidic protein (GFAP), and microglia marker ionized calcium-binding adapter molecule 1 (Iba1) was performed.

## METHODS

### *Experiment 1: To determine if the sex difference in cell addition to the rat AVPV is due to greater cell proliferation or survival in females*

#### Animals and Experimental Design

A total of 42 male and 42 female weanling female Sprague-Dawley rats (P21) were ordered from Harlan and double-housed with same-sex cage mates in 37.5 x 33 x 17 cm clear polycarbonate cages with *ad libitum* access to food (Teklad Rodent diet no. 8640; Harlan,

Madison, WI) and water. They were maintained on a 14:10 light:dark cycle (lights off at 1300 h). On P30, rats received an ip injection of BrdU at a dose of 200 mg/kg dissolved in sterile saline (20 mg/ml) at ~ 0800 h, 1600 h, and 2400 h. Rats were perfused 2 d, 4 d, 7 d, 14 d, 21 d, or 42 d after the final BrdU injection. All perfusions (n=7/ time point) took place at approximately 1300 h (lights out). Animals were treated in accordance with the National Institutes of Health's Guide for the Care and Use of Laboratory Animals. Michigan State University's Institutional Animal Care and Use Committee approved all protocols.

**Perfusions and Sectioning**

Animals were sacrificed with an overdose of sodium pentobarbital (90 mg/kg, ip) and transcardially perfused with 0.9% buffered saline rinse (pH 7.4) followed by 4% paraformaldehyde in cold 0.1 M phosphate buffered saline. Brains were removed and post-fixed in 4% paraformaldehyde overnight (approximately 18 hours), transferred to 30% sucrose for 1 week, and sectioning began once the brains had sunk. Brains were cryostat-sectioned at 30 µm and placed into cryoprotectant solution at -20°C. The left hemisphere of the cortex was marked using a 26 g needle. One set of sections (1-in-12 series) was mounted onto subbed glass slides and Nissl-stained.

**Single-label BrdU immunohistochemistry**

A 1-in-6 series of free-floating sections was immunohistochemically processed for BrdU by procedures described previously (Mohr and Sisk, 2013), with minor modifications. Rinses and incubations with reagents were conducted at room temperature unless otherwise noted. Free-floating sections were rinsed in Tris-buffered saline (TBS; 0.05 M). Endogenous peroxidase

activity was eliminated by incubation in 0.6% $H_2O_2$ for 30 min. Sections were placed in 1.86 N HCl for 30 min at 37 °C, and then rinsed for 10 min in borate buffer (0.1 M; pH 8.5). The tissue was blocked in AffiniPure Fab Fragment donkey anti-rat IgG (Jackson ImmunoResearch, cat no. 712-007-003, working concentration 12 µg/ml) in TBS with 0.1% triton-x-100 and 3% donkey serum for 30 minutes, then incubated overnight at 4 °C in monoclonal primary antibody rat anti-BrdU (catalog no. MCA2060; Serotec) at a working concentration of 1 µg/mL. Sections were incubated for 2 h in Biotin-SP-conjugated AffiniPure donkey anti-rat secondary antibody (cat no. 712–065-150; Jackson ImmunoResearch) at a working concentration of 2 µg/mL, then for 60 min with avidin/ biotinylated enzyme complex reagent (ABC Elite Kit; Vector Laboratories), and reacted with 3,3′-diaminobenzidine tetrahydrochloride (Sigma-Aldrich, catalog no. D5905; 0.25 mg/ml) with 0.012% hydrogen peroxide in 0.05 TBS for 2 minutes. After mounting the tissue onto glass slides, slides were coverslipped using Vectashield mounting medium with DAPI (Vector H-1200) and stored at 4°C. BrdU-positive control tissue was used to confirm BrdU-ir, and consisted of tissue from a 1.5-2 month old rat whose dam received BrdU during the latter end of gestation. Controls excluding primary or secondary antibodies were run using experimental tissue that did not contain the AVPV. Microscopic examination of control sections revealed little to no nonspecific background staining.

**Microscopic Analyses and Quantification of Single-Label BrdU**

To analyze the total number of BrdU-ir cells in the AVPV of female and male rats, 4 anatomically matched sections of the AVPV were selected from a 1-in-6 series. Analyses were performed on an Olympus BX51 microscope with brightfield illumination, as well as epi-illumination (mercury arc lamp with DAPI filter) using Neurolucida software (MBF Bioscience;

Williston, Vermont). The AVPV was located and traced bilaterally using DAPI counterstain at 100x magnification. A 1-in-12 series of Nissl-stained sections also served as a guide for tracing AVPV. BrdU-ir cells were counted at 400x magnification using an UPlanSApo 40x (0.9 NA) objective.

**Statistical Analyses**

ANOVA with Bonferroni post-hoc tests were performed to determine if the total number of BrdU-ir cells in 4 anatomically matched sections of the AVPV differed between sexes and as a function of cell age (i.e. days post-BrdU injection). Thus, the dependent variable was total number of BrdU-ir cells and the independent variables were sex (female, male) and cell age (2, 4, 7, 10, 14, 21, and 42 d).

***Experiment 2: To determine if BrdU is incorporated into proliferating, not dying, cells in the AVPV.***

**Animals and Experimental Design**

Thirty-six female weanling female Sprague-Dawley rats (P23) were ordered from Harlan and singly housed in 37.5 x 33 x 17 cm clear polycarbonate cages with *ad libitum* access to food (Teklad Rodent diet no. 8640; Harlan, Madison, WI) and water. They were maintained on a 14:10 light:dark cycle (lights off at 1300h). On P30, rats were given a single intraperitoneal (ip) injection of 5-bromo-2'-deoxyuridine (BrdU, Sigma-Aldrich) at a dose of 200 mg/kg, dissolved in sterile saline (10 mg/ml solution) between 1200-1400h. Rats were perfused 2 h, 4 h, 1 d, 2 d, 4 d, 7 d, 10 d, 14 d or 21 d after BrdU injection. With the exception of the 2 h and 4 h post-BrdU

perfusion groups, all perfusions (n = 4/timepoint) took place at approximately 1500h (2 h after lights off).

**Perfusions and Sectioning**

Animals were sacrificed with an overdose of sodium pentobarbital (90 mg/kg, ip) and transcardially perfused with 0.9% buffered saline rinse (pH 7.4) followed by 4% paraformaldehyde in cold 0.1 M phosphate buffered saline. Brains were removed and post-fixed in 4% paraformaldehyde overnight (approximately 18 hours) and transferred to 30% sucrose for 1 week, and sectioning began once the brains sunk. Brains were cryostat-sectioned at 40 µm and placed into cryoprotectant solution at -20°C. The left hemisphere of the cortex was marked using a 26 g needle. One set of sections (1-in-4 series) was mounted onto subbed glass slides and Nissl-stained.

**Double-label PCNA/BrdU immunofluorescence**

In order to determine if BrdU was indeed incorporated into proliferating cells and not cells undergoing DNA repair or apoptosis, labeling with BrdU and proliferating cell nuclear antigen (PCNA), which is only expressed during the synthesis phase of the cell cycle, was performed. Tissue containing the AVPV from animals perfused 2 h, 4 h, 1 d, 2 d, 4 d, 7 d, 10 d, 14 d, or 21 d after BrdU injection (n = 2-3/ timepoint) was processed for BrdU/PCNA fluorescent labeling. After rinses in 0.05M TBS, sections underwent antigen retrieval via incubation in 0.01M citric acid, pH 6.0, for 10 min at 95°C and were then cooled for 30 min at room temperature. Sections were then incubated in 0.6% $H_2O_2$ for 30 min. After a 2 h incubation at 65°C in 50% formamide in SSC buffer, sections were rinsed in SSC for 15 minutes, incubated for

30 min in 2 N HCl, and then rinsed in 0.1M borate buffer (pH 8.5) for 10 min. Tissue was blocked in 0.1% Triton-X-100 and 3% goat serum (Chemicon, S 26-100) in TBS for 30 min, then incubated for 72 hrs at 4°C in monoclonal rat anti-BrdU (Serotec, MCA2060, 1:1000 dilution, working concentration 1 µg/ml) and monoclonal mouse-anti PCNA (Santa Cruz, SC 56, 1:50 dilution, working concentration 4 µg/ml). Subsequently, sections were incubated for 3 h in Alexa Fluor 488 goat anti-rat (Invitrogen, A-11006, 1:250 dilution) and Alexa Fluor 635 goat anti-mouse (Invitrogen, A-31575, 1:250 dilution) in TBS and 0.2% Triton-x-100. Sections were thoroughly rinsed in TBS before and between all incubations. After the last rinse, sections were mounted onto glass slides, coverslipped using Vectashield mounting medium with DAPI (Vector H-1200) and stored at 4°C. BrdU-positive control tissue was used to confirm BrdU-ir, and consisted of tissue from a 1.5-2 month old rat whose dam received BrdU during the latter end of gestation. Controls excluding primary or secondary antibodies were run using experimental tissue that did not contain the AVPV. Microscopic examination of control sections revealed little to no nonspecific background staining.

**Microscopic Analyses and Quantification of BrdU/PCNA colocalization**

Z stacks containing BrdU-ir cells in the AVPV were taken with a Leica DMR microscope under epi-illumination using MBF Bioscience's Image Stack Module for Neurolucida. Stacks were taken at 1-micron steps spanning the Z-axis of the cell using an UPlanSApo 40× (0.9 NA) objective. FITC and TRITC filters were used to visualize BrdU- and PCNA-positive cells, respectively. Colocalization was confirmed using the 3D Visualization, and Neurolucida software was used for quantification of cells.

**Statistical Analyses**

To determine if the percent of BrdU-ir cells that colocalize with PCNA-ir in the AVPV differs with time-post BrdU in female rats, a one-way ANOVA was done with cell age (time-post BrdU) as the independent variable and percentage of BrdU-ir cells that colocalized with PCNA-ir as the dependent variable. Significant main effects were followed up with a post-test for a linear trend.

***Experiment 3: To determine if pubertally born cells in the AVPV differentiate into neurons, astrocytes, or microglia in adulthood.***

**Animals and Experimental Design**

Sixteen weanling female Sprague-Dawley rats (P21) were ordered from Harlan and double-housed in 37.5 x 33 x 17 cm clear polycarbonate cages with *ad libitum* access to food (Teklad Rodent diet no. 8640; Harlan, Madison, WI) and water. They were maintained on a 14:10 light:dark cycle (lights off at 1300h). Animals were given a week to acclimate after arrival. During this time, they were handled daily. From P28-P56 rats received a daily intraperitoneal (ip) injection of 5-bromo-2'-deoxyuridine (BrdU, Sigma-Aldrich) at a 200-mg/kg dose, dissolved in sterile saline (20 mg/ml) at approximately 1200 h. Three weeks after the last injection (P77) rats were perfused. Animals were treated in accordance with the National Institutes of Health's Guide for the Care and Use of Laboratory Animals. Michigan State University's Institutional Animal Care and Use Committee approved all protocols.

**Perfusions and Sectioning**

Animals were sacrificed with an overdose of sodium pentobarbital (90 mg/kg, ip) and transcardially perfused with 0.9% buffered saline rinse (pH 7.4) followed by 4% paraformaldehyde in cold 0.1 M phosphate buffered saline. Brains were removed and post-fixed in 4% paraformaldehyde overnight (approximately 18 hours) then transferred to 30% sucrose. Brains were cryostat-sectioned at 30 µm, and sections were placed into cryoprotectant solution at -20°C. During sectioning, the left hemisphere of the cortex was marked using a 26-gauge needle.

**Triple-label BrdU/GFAP/NeuN Immunofluorescence**

To determine if pubertally born cells in the female rat AVPV differentiate into astrocytes or neurons, triple-label immunofluorescence for BrdU, astrocyte marker glial fibrillary acidic protein (GFAP), and mature neuronal marker neuronal nuclei (NeuN) was performed. The methods were completed as previously described (Mohr and Sisk, 2013), with minor changes. A 1 in 3 series of free-floating sections were incubated in 0.1% sodium borohydride for 10 minutes to reduce autofluorescence. Sections were incubated in 0.93N HCl for 30 minutes at 37°C followed by a 10-minute incubation in 0.1M borate buffer. Tissue was blocked for 1 hour in TBS-plus (0.3% Triton-X-100 and 6% goat serum in TBS), followed by a 48 hour incubation at 4°C in a primary antibody cocktail solution containing monoclonal rat anti-BrdU (Serotec, cat no. MCA2060; 1:1000 dilution, working concentration 1 µg/ml), monoclonal mouse anti-NeuN (Chemicon, cat no. MAB377, clone A60; 1:1000 dilution, working concentration 1 µg/ml), and polyclonal rabbit anti-GFAP (Dako, cat no. Z0334; 1:5000 dilution, working concentration 0.58

µg/ml) in TBS-plus. Sections were incubated for 2 h in a secondary antibody cocktail solution containing biotin-SP-conjugated AffiPure goat anti-rat (Jackson, cat no. 112 065 003; 1:1000 dilution, working concentration 1.3 µg/ml), Cy3-conjugated AffiniPure Goat anti-rabbit (Jackson, cat no. 111 165 144; 1:500 dilution, working concentration 3 µg/ml) and Alexa Fluor 635 goat anti-mouse (Life Technologies, cat no. A-31574; 1:500 dilution, working concentration 4 µg/ml). The BrdU label was detected with a 1 h incubation in Cy2-conjugated streptavidin (Jackson, cat no. 016 220 084; 1:1000 dilution, working concentration 1.8 µg/ml) and then sections were mounted onto glass slides and coverslipped using SlowFade gold antifade reagent (Life Technologies, cat no. S36936). BrdU-positive control tissue was used to confirm BrdU-ir, and consisted of tissue from a 1.5-2 month old rat whose dam received BrdU during the latter end of gestation. Controls excluding primary or secondary antibodies were run using experimental tissue that did not contain the AVPV. Microscopic examination of control sections revealed little to no nonspecific background staining.

**Double-label BrdU/Iba1 Immunofluorescence**

To determine if pubertally born cells in the female rat AVPV differentiate into microglial cells in adulthood, double-label immunofluorescence for BrdU and microglia marker Iba1 was performed. A 1 in 3 series of free-floating sections was incubated in 0.1% trypsin/0.1% calcium chloride (CaCl2) in 0.1M tris-buffered saline (TBS) for 5 minutes. Tissue was incubated at 37°C in 2N HCl for 30 minutes, followed by a 10-minute incubation in 0.1M borate buffer (pH 8.5). After blocking in 10% bovine serum albumin (BSA; Sigma, cat no. A3733)/ 6% normal goat serum (Pel-Freez, code no. 32130-5)/ 0.4% tween in TBS for 1 hour, tissue was incubated overnight in a primary antibody cocktail solution containing monoclonal rat anti-BrdU (Serotec, cat no.

MCA2060; working concentration 1 µg/ml) and rabbit anti-Iba1 (Wako, cat no. 019-19741; working concentration 1 µg/ml). Tissue then underwent a 2-hour incubation in a secondary antibody cocktail solution containing biotin-SP-conjugated AffiPure goat anti-rat (Jackson, cat no. 112 065 003; working concentration 1.3 µg/ml), Cy3-conjugated AffiniPure Goat anti-rabbit (Jackson, cat no. 111 165 144; working concentration 1.5 µg/ml). The BrdU label was detected with Cy2-conjugated streptavidin (Jackson, cat no. 016 220 084; working concentration 1.8 µg/ml) for 1 hour and then sections were mounted onto glass slides and coverslipped using SlowFade gold antifade reagent (Life Technologies, cat no. S36936). Tissue was rinsed with 0.1M TBS initially and between all incubations, and all incubations took place at room temperature unless otherwise noted. BrdU-positive control tissue was used to confirm BrdU-ir, and consisted of tissue from a 1.5-2 month old rat whose dam received BrdU during the latter end of gestation. Controls excluding primary or secondary antibodies were run using experimental tissue that did not contain the AVPV. Microscopic examination of control sections revealed little to no nonspecific background staining.

**Microscopic Analyses and Quantification**

BrdU/GFAP/NeuN

Confocal Z stacks containing BrdU-ir cells in the AVPV were taken with an Olympus FluoView FV1000 confocal laser-scanning microscope equipped with FV1000 ASW software. Stacks were taken at 0.5-micron steps spanning the Z-axis of the cell using an UPLFLN 40× oil objective (1.3 NA). The multi-line argon laser (488 nm), green HeNe laser (543 nm), and red HeNe laser (633 nm) were used to image BrdU-, GFAP- and NeuN-positive cells, respectively. All

BrdU-ir positive cells were imaged 3-5 sections/animal, yielding 29-52 images of BrdU positive cells/animal for phenotypic analysis. Image stacks were imported into MBF Bioscience's Image Stack Module for Neurolucida, where colocalization was confirmed using the 3D Visualization. Neurolucida software was used for quantification of cells. GFAP red fluorescence was pseudo-colored magenta.

BrdU/Iba1

Z stacks containing BrdU-ir cells in the AVPV were taken with an Olympus BX51 microscope under epi-illumination using MBF Bioscience's Image Stack Module for Neurolucida. Stacks were taken at 0.5-micron steps spanning the Z-axis of the cell using an UPlanSApo 40× (0.9 NA) objective. FITC and TRITC filters were used to visualize BrdU- and Iba1-positive cells, respectively. Red fluorescence was pseudo-colored magenta. Colocalization was confirmed using the 3D Visualization, and Neurolucida software was used for quantification of cells.

## RESULTS

### *Experiment 1: The sex difference in pubertally born cells in the AVPV is due to both greater proliferation and survival in females compared with males.*

Cells are added to the female and male AVPV during early puberty (P30) and many of these cells survive at least 6 weeks (Figure 1.1). The BrdU-ir cells in male and female rats were evenly distributed throughout the AVPV and were not confined to a particular region of the AVPV (i.e., the BrdU-ir cells were not clustered along the lining of the third ventricle). ANOVA with Bonferroni post-hoc tests (Figure 1.1b) were done to determine if the mean total number of BrdU-ir cells in 4 anatomically matched sections of the AVPV differed between females and

males and as a function of days post-BrdU injection. Main effects of sex and days post-BrdU were found, with females having more BrdU-ir cells in the AVPV compared with males ($F(1,53) = 5.065$, $p = 0.029$), and with the mean total number of BrdU-ir cells differing as a function of time post-BrdU ($F(6,53) = 3.518$, $p = 0.005$). Bonferroni post-hoc tests were done to compare the mean total number of BrdU-ir cells at different days post-BrdU injection and revealed that there are significantly more BrdU-ir cells at 7 days compared to 42 days post-BrdU treatment ($p = 0.004$).

To further probe whether the attrition of newly born cells in the AVPV differs between sexes, regression analyses were performed separately by sex. In both sexes, the total number of BrdU-ir cells decreased as a function of time. In males, the slope of the line of best fit was -0.52, $F(1,33) = 11.672$, $p < 0.01$, $\beta = -.0.517$, $b = -0.428$, $R^2 = 0.267$, while in females the line of best fit was -0.42, $F(1,32) = 6.794$, $p < 0.05$, $\beta = -.0.424$, $b = -0.492$, $R^2 = 0.18$. Lines of best fit are superimposed onto the graph in Figure 1.1 and the slope of the lines suggest that the attrition of newly born cells in the AVPV is similar between females and males.

Regression analyses were conducted to determine if the proportion of the BrdU population that was paired decreased as the cells age (i.e. as a function of days post-BrdU), Figure 1.2. BrdU pairs are thought to be indicative of recently divided cells, and pairs within the parenchyma suggest *de novo* cell proliferation (Kokoeva et al., 2007). Analyses were done separately by sex, to determine if the attrition in the proportion of paired BrdU cells differed between males and females. For males, the slope of the line of best fit was -0.6, $F(1,33) = 18.514$, $p < 0.001$, $\beta = -.0.605$, $b = -0.005$, $R^2 = 0.367$, indicating that the proportion of paired

BrdU cells in the male rat AVPV decline as a function of days post-BrdU. Thus in males, each day after BrdU treatment, the proportion of the BrdU population that exists as pairs decreases by 0.005, or 0.5%. For females, the slope of the line of best fit was -0.2, $F(1,32) = 1.03$, $p > 0.3$, $\beta = -0.179$, $b = -0.002$, $R^2 = 0.032$. Thus, the proportion of BrdU cells that are paired in the female rat AVPV is stable 6 weeks after BrdU treatment, indicating that the cells considered to be locally synthesized in the parenchyma of the AVPV survive in females, but not in males.

***Experiment 2: BrdU is incorporated into proliferating cells in the AVPV***

Two hours post- BrdU injection, 94.44 ± 5.55 % of BrdU-ir cells colocalize with PCNA-ir, indicating that BrdU is incorporated into proliferating, not cells undergoing DNA repair in the AVPV. ANOVA revealed a significant main effect of cell age/time post-BrdU ($F(7,11) = 3.071$, $p = 0.0472$. Post-test revealed a significant linear trend ($p = 0.0082$, $R^2 = 0.32$, slope = -4.19), indicating that the percent of BrdU-ir cells that colocalize with PCNA-ir decreases as the cells age. Note that at 7, 10, and 14 d there are some BrdU-ir cells that colocalized with PCNA-ir, indicating that these cells were proliferating on the day of perfusion. It is possible that these cells are the daughter or granddaughter cells of a cell that was born on the day of BrdU injection and indicates a second wave of proliferation. However, it should be noted that because only one systemic BrdU injection was given, the actual number of BrdU-ir cells was low (i.e. an average of 5 BrdU-ir cells/animal/timepoint). In this case 0% colocalization could mean that 0/1 BrdU-ir cells expressed PCNA-ir, thus indicating a floor effect.

### *Experiment 3: Some pubertally born cells in the female rat AVPV differentiate into neurons, astrocytes, and microglial cells*

When BrdU was injected every day for 4 weeks during puberty (P28-P56), 57% of the cells had differentiated into mature neurons, astrocytes, or microglial cells when examined on P77. Thus, the newborn cells observed in the AVPV were anywhere from 3-7 weeks old. Throughout anatomically matched sections of the AVPV, stacks containing BrdU-ir cells were taken and examined for colocalization with mature neuronal marker NeuN, astrocyte marker GFAP, or microglia marker Iba1. While 43 ± 2% of BrdU-ir cells did not colocalize with any of the three markers, 15 ± 2% colocalized with NeuN, 19 ± 2% colocalized with GFAP, and 23 ± 3% colocalized with Iba1. In figure 1.4, circular histograms depict the proportion of BrdU-ir cells that co-labeled with Iba1, GFAP, or NeuN.

## DISCUSSION

This study established that neurogenesis, gliogenesis, and microgliogenesis occur in the female rat AVPV throughout puberty. Furthermore, the sex difference in the number of pubertally born cells in the rat AVPV is due to greater cell addition in females compared to males.

### *Female-biased sex difference in number of pubertally born cells in the rat AVPV*

These data confirm a female-biased sex difference in the number of cells added to the AVPV during early puberty. These data extend previous findings and suggest that this sex difference is not due to greater cell death in males, but that females initially have more cells

added to the AVPV compared to males. Some of these pubertally born cells die as they age, but there are no sex differences in attrition of pubertally born cells in the AVPV.

Indeed, cell death is an important mechanism that establishes and maintains sex differences in cell density and the volume of the AVPV (Ahern et al., 2013; Forger et al., 2004; Waters and Simerly, 2009; Zup et al., 2003). During early postnatal development (i.e. from P1-P5) there is a high amount of cell death within the AVPV in both sexes, indicated by activated caspase-3 immunohistochemistry, but there is no sex difference in cell death in the AVPV from P1-P11 (Ahern, 2013). On embryonic day 21, males have more pyknotic cells in the AVPV compared to females, but female fetuses exposed to testosterone propionate (TP) from days 14-18 of gestation have the same number of pyknotic cells in the AVPV compared with males, thus prenatal testosterone increases cell death in the AVPV (Sumida, 1993). Overexpression of anti-apoptotic protein Bcl-2 (Zup et al., 2003) and deletion of pro-apoptotic protein Bax (Forger et al., 2004) eliminates the sex difference in volume and cell density of the AVPV in adulthood. Thus, there is an organizing effect of prenatal testosterone on cell death, where testosterone increases prenatal cell death in the AVPV. Sex differences in developmental cell death help establish morphological sex differences in the AVPV, but that is only half of a two-sided coin. Cell addition must also be considered as a means of *maintaining* morphological sex differences. If cell death occurs in the AVPV throughout life without a turnover of cells, conceivably one would expect an age-related decline in the volume of the AVPV. Such is not the case—there are no differences in AVPV volume between young (3-4 month), middle age (10-12 month), and old (24-26 month) female rats (Chakraborty et al., 2003). Interestingly, the sex difference in AVPV volume does not appear until after puberty (Davis et al., 1996). Therefore, it seems that

hormone-dependent cell death during the prenatal period establishes morphological sex differences in the AVPV while hormone-dependent cell addition along with cell death after puberty maintains these sex differences.

***BrdU is incorporated into proliferating cells in the female rat AVPV***

About 15% of newly born cells in the rat AVPV appeared as pairs in the parenchyma, indicative of *de novo* production of newly born cells (Kokoeva et al., 2007). Thus, not all newly born cells are migrating into the AVPV from the classical neurogenic zones (i.e. the subventricular zone (SVZ) of the lateral ventricle and the subgranular zone (SGZ) of the hippocampus). In general, the hypothalamus has been established as a third neurogenic zone of the brain (for reviews see (Cheng, 2013; Migaud et al., 2010), with implications in energy balance regulation (Kokoeva, 2005; Lee et al., 2012; Pierce and Xu, 2010) and reproduction (Cheng et al., 2011). The presence of paired BrdU cells in the hypothalamic parenchyma suggests that cells are proliferating within the AVPV during early puberty. Interestingly, in males the proportion of BrdU cells that were paired decreased across time, while in females the proportion of paired BrdU cells remained stable. Because the proportion of BrdU pairs did not significantly decline from 2 up to 42 days after BrdU treatment in female rats, it seems that the cells produced within the parenchyma are slated for survival in females, but not males.

BrdU-labeled cells were present in the female AVPV 2 hours following BrdU injection, and 94% of these cells expressed cellular proliferation marker PCNA, validating the use of BrdU as a cell birthdating marker and indicating that these are indeed newly born cells. Because 2 hours is not enough time for a new cell to move from the SVZ or the SGZ into the AVPV, these new cells could be coming from the third ventricle, given that the ependymal layer contains

neural progenitor cells (Xu et al., 2005); for review see (Rojczyk-Golebiewska et al., 2014). Together, these data provide compelling evidence that cell proliferation occurs within the AVPV during early puberty in the female rat.

***Pubertal neuro- and gliogenesis in the female rat AVPV***

Fifteen percent of pubertally born cells in the female AVPV differentiated into neurons, 20% into astrocytes, and 23% into microglia, demonstrating pubertal neurogenesis and gliogenesis in the female rat AVPV. The percentage of pubertally born cells that differentiate into neurons and astrocytes in the AVPV is similar to previous studies that phenotyped pubertally born cells in limbic and hypothalamic regions of male hamsters (Mohr and Sisk, 2013).

Astrocytes within the AVPV play an important role in estrogen positive feedback and the generation of the preovulatory LH surge. Estrogen positive feedback involves an intricate dance between hypothalamic astrocytes in the AVPV, which synthesize progesterone (neuroP) in response to estrogen through membrane estrogen receptor-α (mERα) signaling and kisspeptin neurons (Bondar et al., 2009; Kuo et al., 2010a; Micevych et al., 2003a; Sinchak et al., 2003). The AVPV kisspeptin neurons integrate estradiol and progesterone signaling to stimulate release of a surge of gonadotropin-releasing hormone (GnRH), which in turn stimulates the LH surge from the pituitary, triggering ovulation. Observations from the Micevych laboratory indicate that astrocytes harvested from prepubertal mice do not synthesize neuroP in response to estradiol administration (Micevych et al., 2007), and maturation of these astrocytes in vitro did not make them competent to respond to estradiol. This is in contrast to astrocytes harvested from adult female, but not male mice, which do respond to estradiol by synthesizing

neuroP (Kuo et al., 2010a). In rodents, estrogen positive feedback that triggers the LH surge only occurs in females after puberty (Andrews et al., 1981; Hoffman et al., 2005). It is tempting to speculate that the birth of estrogen-sensitive astrocytes in the AVPV during puberty contributes to the gain of function in brain circuits that control estrogen positive feedback, but more work needs to be performed to determine if this is the case.

Aside from the starring role that astrocytes play in estrogen positive feedback by neuroP secretion, glial cells play an important supporting role in gonadal steroid feedback and reproductive neuroendocrine output (for review, see (Garcia-Segura et al., 2008)). In 3-4 month old rats, astrocytes in the rostral preoptic area that are apposed to GnRH neurons exhibit hormonally mediated fluctuations in morphometry such that the amount of GnRH surface area covered by astrocytic processes decreases just before the initiation of the preovulatory GnRH/LH surge, likely allowing increased synaptic input to GnRH neurons (Cashion et al., 2003). Pubertally born astrocytes in the female rat AVPV could be these astrocytes that interact with GnRH neurons. Astrocytes also release an assortment of factors that promote GnRH release. Of these, growth factors of the epidermal growth factor (EGF) family play a crucial role in glia-to-GnRH neuron and glia-to-glia communication that results in GnRH secretion (for reviews see (Dhandapani et al., 2003; Ojeda et al., 2010)). Whether pubertally born astrocytes in the female rat AVPV release growth factors important to GnRH release remains to be elucidated.

While microglial cells have typically been thought of as the resident immune cells of the brain, new evidence suggests that these cells also play roles in regulatory processes such as cell proliferation and survival, programmed cell death, synaptogenesis, and synaptic pruning (for review, see (Lenz and McCarthy, 2015)). Microglia are now known to be critically involved in

sexual differentiation of the male biased preoptic area (POA) of the hypothalamus and male mating behavior (Lenz et al., 2013), and their function in the female rodent AVPV during puberty may be similarly involved in sexual differentiation and female reproduction. It is important to remember that the cells colocalizing BrdU and Iba1 seen in the current study are cells that are anywhere from 3-7 weeks old. Microglia acting in a classical manner, e.g., activated in response to neuroinflammation, die within a day of a neuroimmune challenge (Vazquez-Villoldo et al., 2014), suggesting that the microglia in the current study are perhaps involved in regulatory processes, and not macrophagic processes. Indeed, even "resting" microglia are actually quite active, as they extend and retract their processes within minutes to survey their environment (Nimmerjahn et al., 2005). Pubertally born microglia could be major players in maintaining the morphological sexual dimorphism in the AVPV, and the results of the current study warrant further investigation into the role that pubertally born microglia in the female rat AVPV play in sexual differentiation.

The remaining 43% of BrdU-ir cells that did not colocalize with any of the phenotypic markers could be a combination of undifferentiated precursor cells, immature neurons not yet expressing NeuN, and mature neurons that do not express NeuN. The use of NeuN as a pan marker of mature neurons has been met with limitations. NeuN expression varies even within different subregions of brain nuclei (Snyder et al., 2012), so it is likely that newly born cells in the AVPV require a longer amount of time to express NeuN. The BrdU/NeuN colocalized cells observed in the present study could be cells born during the first couple weeks of puberty, while the cells born during the latter half of puberty might not have had enough time to differentiate into mature neurons. The youngest BrdU cell in the present study would have

been 3 weeks old, and in the dentate gyrus of the hippocampus, between 40 and 80% of 3-week-old BrdU-ir cells expressed NeuN-ir (Snyder et al., 2012). Another limitation of NeuN as a marker of mature neurons is that not all neuronal populations express NeuN, including cerebellar Purkinje cells, olfactory bulb mitral cells, and retinal photoreceptor cells (Mullen et al., 1992). Furthermore, loss of NeuN antigenicity has been demonstrated in the spinal cord with aging (Portiansky et al., 2006) and after cerebral ischemia (Unal-Cevik et al., 2004), indicating that a lack of NeuN staining could be a false negative. Thus, the current estimates of pubertally born neurons are conservative, but even if NeuN correctly labeled neurons, the population of undifferentiated cells or immature neurons could be playing a supporting role.

***Conclusion***

This study documents that cell addition to the AVPV during puberty contributes to the maintenance of morphological sex difference in the AVPV, and that the pubertal female AVPV is an environment rich in neuro- and gliogenesis. These results highlight the preoptic area as another neurogenic zone of the brain.

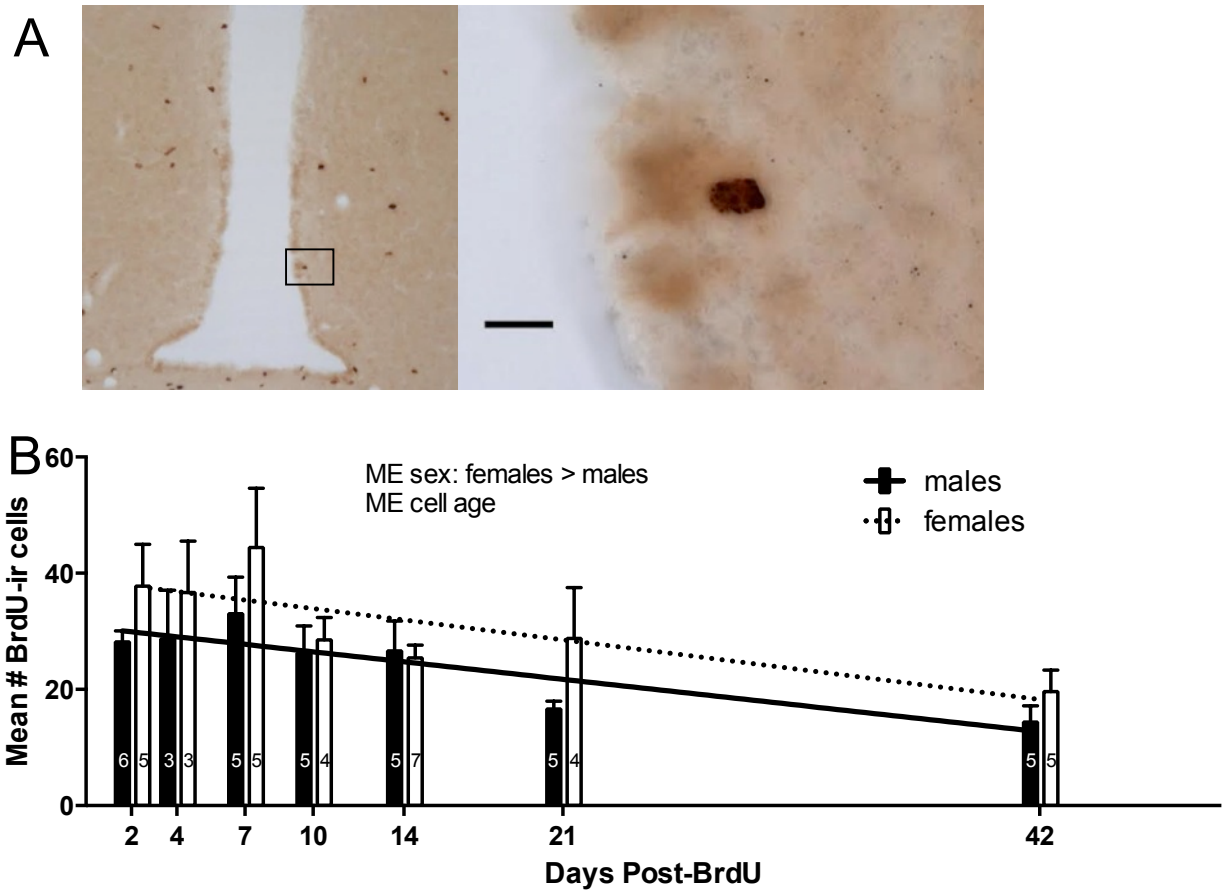


**Figure 1.1: The sex difference in pubertally born cells in the AVPV is due to greater proliferation in females compared to males- experiment 1.**

(A) Representative photomicrographs of BrdU-labeled cells in the AVPV at low and high power, respectively. Brightfield images were taken using a 10x and 100x objective, respectively. Boxed area in left image indicates location of right image. Scale bar in right image indicates 10 µm. (B) Graph representing the mean total # of BrdU-ir cells in the AVPV of 4 anatomically matched sections. ANOVA with Bonferroni post-hoc tests revealed two main effects on the mean total # of BrdU-ir cells: 1) sex, where females have more BrdU-ir cells in the AVPV compared with males ($F(1,53) = 5.065$, $p = 0.029$); 2) days post-BrdU ($F(6,53)= 3.518$, $p = 0.005$), where Bonferroni post-hoc tests indicated that total # of BrdU-ir cells in the AVPV was significantly higher 7 days after BrdU compared to 42 after BrdU treatment($p = 0.004$). Graph represents means + SEMs, lines indicate line of best fit from regression analyses, and numbers inside bars indicate n. ME= main effect.

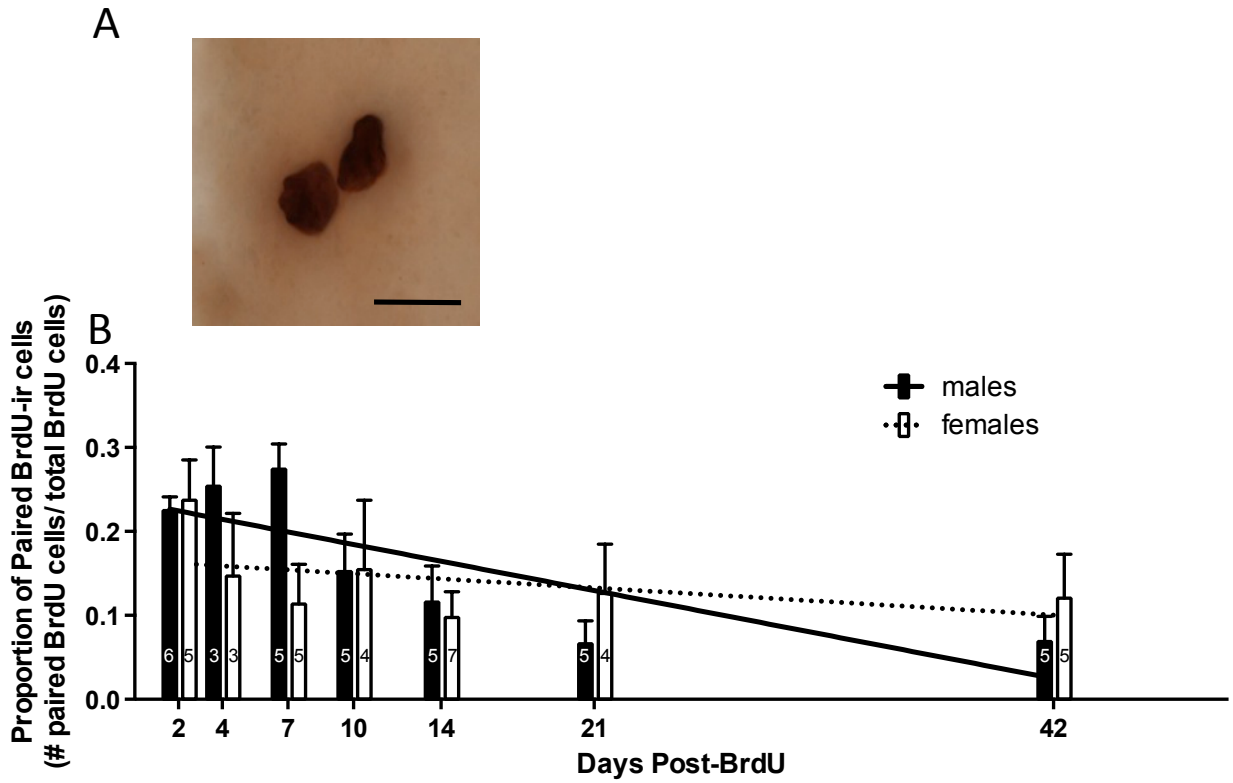


**Figure 1.2: Some BrdU-ir cells in the AVPV are paired-experiment 1.**

(A) Photomicrograph showing a pair of BrdU-ir cells in the AVPV. Image is a minimum intensity projection of 30 images (15 µm thick, 0.5 µm step) taken using a 100x oil objective. Black scale bar indicates 10 µm. (B) Mean proportion of BrdU-ir cells that are paired (+ SEMs). Regression analyses determined that the proportion of paired BrdU cells decreases as a function of time in males ($F(1,33) = 18.514$, $p < 0.001$, $\beta = -.0.605$, $b = -0.005$, $R^2 = 0.367$), but not females ($F(1,32) = 1.03$, $p > 0.3$, $\beta = -0.179$, $b = -0.002$, $R^2 = 0.032$). Lines indicate slope. Numbers inside bars indicate n.

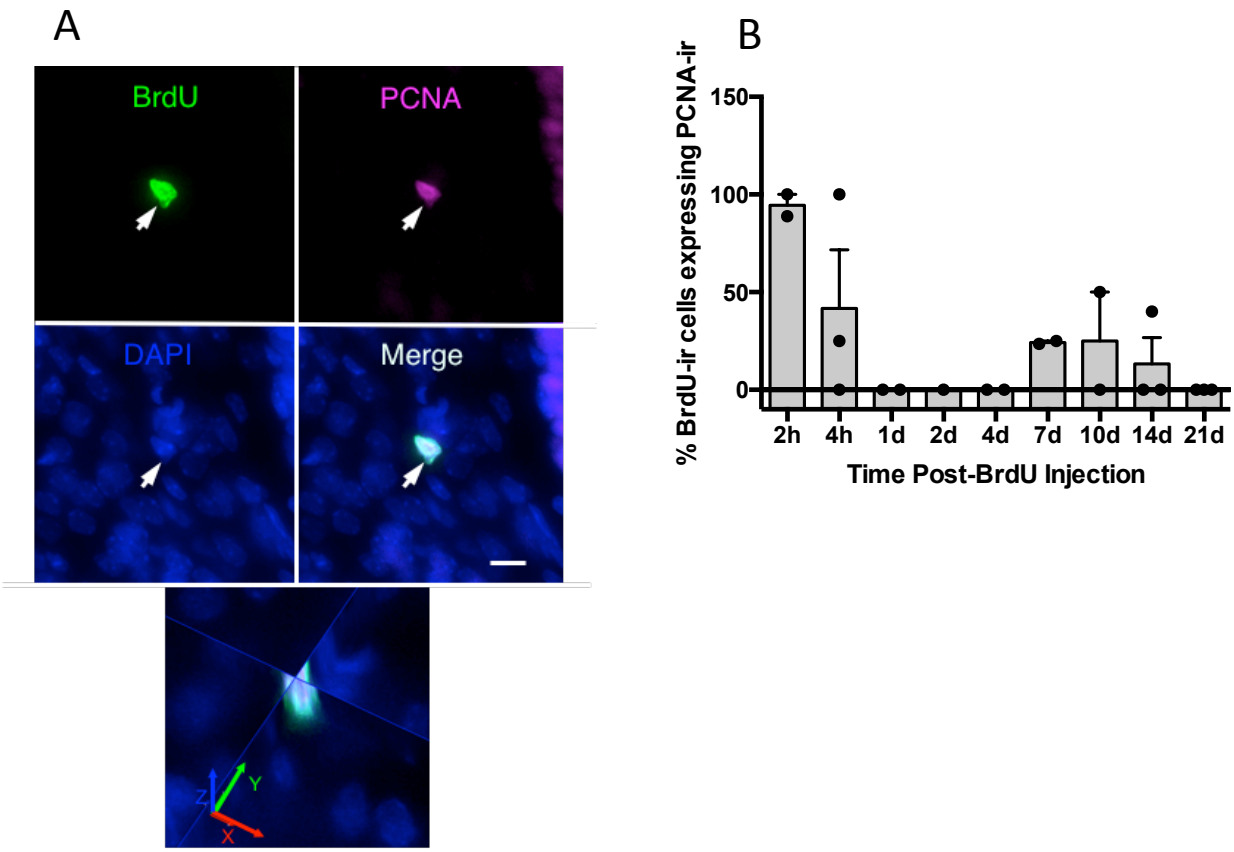


**Figure 1.3: BrdU is incorporated into proliferating cells in the AVPV-experiment 2.**
(A) Z-stack images of BrdU-ir cells colocalized with PCNA-ir in the AVPV. BrdU, PCNA, DAPI, and Merge images are maximum intensity projections of 20 images (20 µm thick, 1 µm step). White scale bars represent 10 µm. Orthogonal view through the middle of the cell confirms colocalization; the red arrow signifies the x plane, green arrow the y plane, and blue arrow the z plane. (B) Mean percent of BrdU-ir cells that express PCNA-ir. Black circles represent individual data. Graph represents means + SEMs.

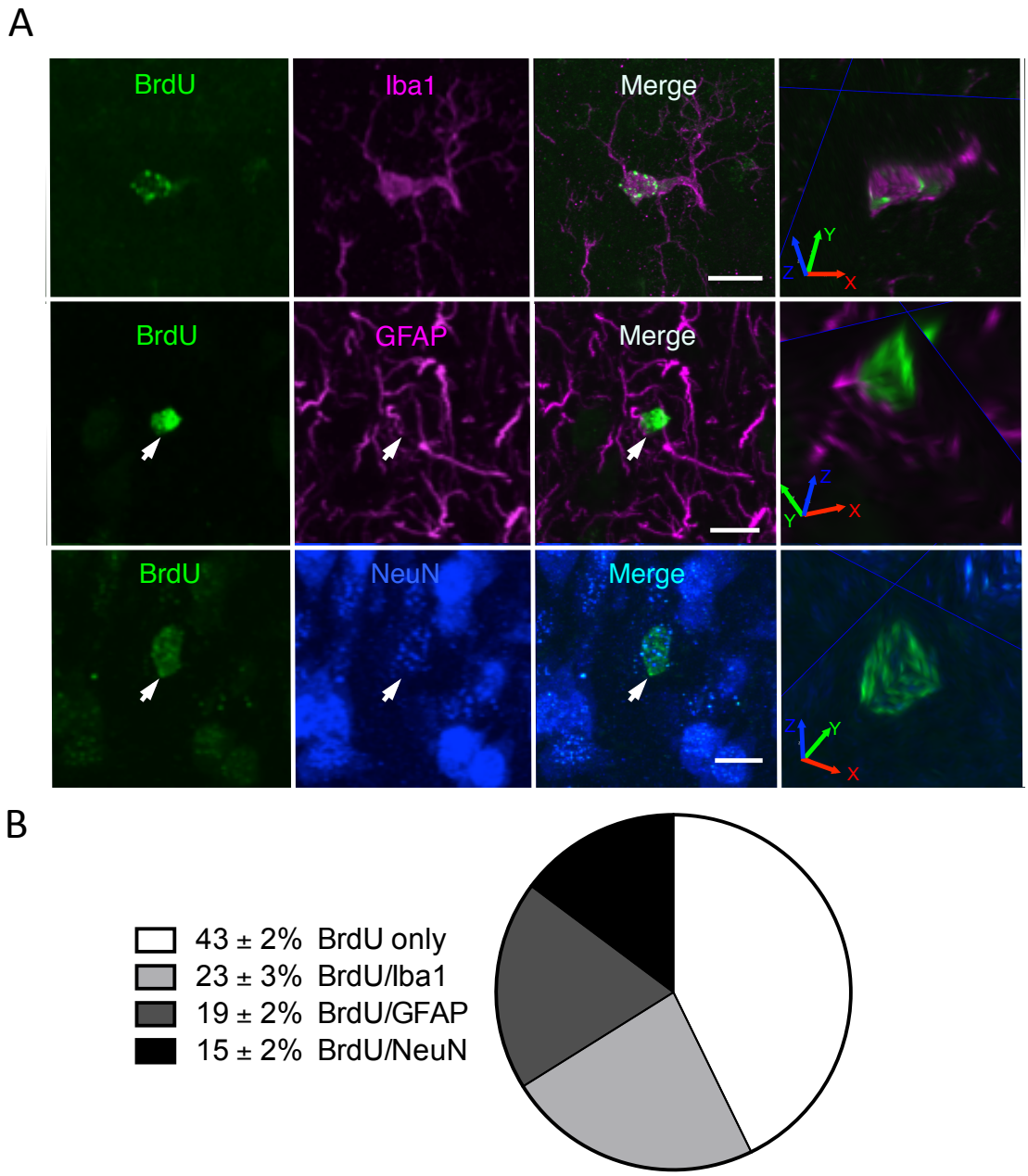


**Figure 1.4: Pubertally born cells in the female rat AVPV differentiate into neurons, astrocytes, and microglia-experiment 3.**

(A) Z-stack images of a BrdU-ir cells colocalized with Iba1-, GFAP-, and NeuN-ir in the AVPV. BrdU, Iba1/GFAP/NeuN, and Merge images are maximum intensity projections of 30 images (15 µm thick, 0.5 µm step). White scale bars represent 10 µm. Orthogonal view through the middle of the cell confirms colocalization; the red arrow signifies the x plane, green arrow the y plane, and blue arrow the z plane. (B) Graphs represent the mean proportion of BrdU-ir cells that express neither label (BrdU only), or that also express Iba1-ir, GFAP-ir, or NeuN-ir (n=6; means ± SEM).

## CHAPTER 2

Functionality of Pubertally Born Cells in the Female Rat AVPV: Involvement in the LH Surge

## INTRODUCTION

The anteroventral periventricular nucleus (AVPV) is a critical component of the preovulatory surge of gonadotropin releasing hormone (GnRH) and luteinizing hormone (LH) that causes ovulation, a pivotal event in reproduction (Petersen and Barraclough, 1989; Wiegand and Terasawa, 1982). The ability of female, but not male, rodents to generate a preovulatory GnRH/LH surge reflects a sexually differentiated neuroendocrine response of the HPG axis that is governed by the AVPV, while the function of the AVPV in males is unknown. Additionally, the AVPV is sexually dimorphic in structure, where it is larger and more cell-dense in females compared to males (Bleier et al., 1982; Davis et al., 1996), and these morphological sexual dimorphisms are not apparent until after puberty (Davis et al., 1996).

The induction of the GnRH/LH surge in female rats normally involves a positive-feedback response to estradiol (E) and progesterone (P), and can only be elicited after puberty. In contrast, male rats given these hormones are unable to elicit a LH surge, regardless of age (Hoffman et al., 2005). Neural activity in this process is reliably correlated with immediate early gene (IEG) *c-fos* and protein product Fos expression in GnRH neurons following estrogen and progesterone treatment in females, but not males (Hoffman et al., 1990; Hoffman et al., 1993; Hoffman et al., 2005). Fos expression in GnRH neurons during the afternoon of proestrus corresponds to LH release, and Fos expression is also seen in the AVPV (Lee et al., 1990). Because this process can only be elicited after puberty, it suggests that during puberty there are changes to the underlying neural circuit that controls the LH surge.

Notably, it is not understood what is different between a prepubertal female rodent and an adult female rodent (male rodents do not have estrogen positive feedback) to allow estrogen positive feedback to occur (i.e. what events happen during puberty that allows maturation and activation of estrogen positive feedback). GnRH mRNA reaches adult levels well before the onset of puberty in male and female mice (Gore et al., 1999) and GnRH is released at high frequencies from the late embryonic period through the first week of postnatal life (Glanowska et al., 2014). Furthermore, GnRH minisurges occur on the afternoon of proestrus in peripubertal rats (Sisk et al., 2001). Together, these findings demonstrate that the GnRH neuronal network is capable of release before puberty, but that it must wait for the appropriate signal during puberty. Kisspeptin is the known stimulator of GnRH release that allows for the onset of puberty and estrogen positive feedback (for review see (Kauffman and Smith, 2013)). Kisspeptin neuron number increases dramatically from P20 to adulthood in the mouse AVPV (Mayer et al., 2010) and this population of neurons that express Kiss1 mRNA in the AVPV is larger in females compared to males (Kauffman, 2010). Concurrently, during puberty new cells are added to the AVPV in a sexually dimorphic manner, where female rats have more pubertally born cells in the AVPV compared to males. Gonadectomy prior to puberty decreases pubertal cell addition in the female rat AVPV to the same level as males, and prepubertal castration has no effect on cell addition in the male AVPV (Ahmed et al., 2008). Thus, there is a hormonally mediated sex-specific addition of cells to the AVPV during puberty, while at the same time the AVPV begins to control a hormonally mediated sexually differentiated response in GnRH release. Whether pubertally born cells in the female rat AVPV play a role in estrogen positive feedback and the GnRH/LH surge remained unknown.

In the present study, we determined whether pubertally born cells in the AVPV were involved in sex-specific gain of function during puberty. First, cell birthdate marker bromodeoxyuridine (BrdU) was given to female rats throughout puberty. In adulthood, females were ovariectomized then hormone-primed to elicit an LH surge, then the brains were taken out at a time when Fos expression is high, corresponding to the LH surge. BrdU/Fos colocalization revealed that around 30% of pubertally born cells were active during the LH surge. Next, to determine if specifically pubertally born cells were necessary for the LH surge, mitotic inhibitor cytosine arabinofuranoside (AraC) was given to female rats during puberty, or for an equal amount of time during early adulthood. A few weeks after the end of AraC treatment females, HPG function was determined by measuring the females' ability to produce an LH surge. AraC treatment and knockdown of cell addition for 4 weeks during puberty or during early adulthood diminished the LH surge. These results suggest that cell addition to the AVPV during puberty and early adulthood is an active mechanism for maintaining HPG axis function, measured by LH output.

## METHODS

### *Experiment 1: To determine the timing of the LH surge following hormone-priming*

#### Animals and Experimental Design

While LH surges have been elicited in rodents in a laboratory setting for decades, many factors affect the exact timing of the LH surge, such as the light:dark cycle and specific hormone regimen. Thus, it was necessary to determine the timing of the LH surge in our colony, on our light cycle, and using our hormone-priming protocol. To do this, 6 adult female Sprague-Dawley rats (between P60-P70) were ordered from Harlan and double-housed in 24 x 46 x 20 cm clear

polycarbonate cages with *ad libitum* access to food (Teklad Rodent diet no. 8640; Harlan, Madison, WI) and water. They were maintained on a 14:10 light:dark cycle (lights off at 1600 h). Animals were given a week to acclimate after arrival. During this time, they were handled daily.

A week after arrival, animals were ovariectomized and femoral catheters (Alzet, custom-made rat femoral catheters) were inserted. Following catheter placement, animals were tethered and singly housed in a larger cage, either 37.5 x 33 x 17 cm, or 51.5 x 41 x 20 cm. After recovering from surgery for 1 week, an LH surge was induced with estradiol benzoate (EB) and progesterone (P; see below). Blood was collected (200 µl) every hour starting the morning of P treatment, at 0800 h. During the expected time of the surge, starting at 1100 h, blood was collected every 20 minutes until 1300 h, and at that point blood was collected every hour until 0300 h. During each blood collection, 200 µl of sterile saline was replaced back into the catheter.

The peak of the LH surge was determined (post-P-treatment) via LH radioimmunoassay (below). About a month after the induction of the LH surge, two more surges were induced. Finally, 4 of the animals were EB- and P- primed (see below), while the other 2 were give sesame oil, and all animals were then transcardially perfused 1 h after the expected time of the surge, at approximately 1600 h (lights out).

**Induction of the LH surge**

Female rats were injected with EB (10 µg in 0.05 ml of sesame oil, subcutaneous injection) for two consecutive days at 1000 h. On the third day, animals received a P injection (500 µg in 0.1 ml sesame oil, subcutaneous injection) at 1045 h.

**Perfusions and sectioning**

Animals were sacrificed with an overdose of sodium pentobarbital (90 mg/kg, ip) and transcardially perfused with 0.9% buffered saline rinse (pH 7.4) followed by 4% paraformaldehyde in cold 0.1 M phosphate buffered saline. Brains were removed and post-fixed in 4% paraformaldehyde overnight (approximately 18 hours) and transferred to 30% sucrose in 0.1M PBS. Brains were cryostat-sectioned at 30 μm, placed into cryoprotectant solution and stored at -20°C. The left hemisphere of the cortex was marked using a 26g needle. One set of sections (1-in-4 series) was mounted onto subbed glass slides and Nissl-stained.

**Single-label Fos Immunohistochemistry**

To determine if there is Fos (a marker of cellular activation) expression in the AVPV following hormone priming, immunohistochemistry for Fos was performed on a 1-in-4 series of free-floating tissue sections containing the AVPV. Tissue was rinsed with 0.05 M tris-buffered saline (TBS) in between all steps, and all incubations took place at room temperature, unless otherwise noted. Tissue was incubated in 1% hydrogen peroxide and 0.3 % triton-x-100 for 10 minutes, then blocked with 20% normal goat serum in TBS + 0.3 % triton-x-100, then incubated in Fos rabbit anti-c-Fos primary antibody (Santa Cruz, sc-52; 1:10,000 dilution, working concentration 1 μg/ml) for 48 h at 4°C. After a 1-hour incubation in biotinylated goat-anti-rabbit IgG (Vector, BA-1000; 1:500 dilution, 3 μg/ml working concentration), tissue was incubated for 1 hour in avidin/ biotinylated enzyme complex reagent (ABC Elite Kit; Vector Laboratories). Tissue was reacted with 3,3'-Diaminobenzidine tetrahydrochloride (DAB; Sigma, D5905; 0.25 mg/ml) with 0.012 % hydrogen peroxide in 0.05 TBS for 2 minutes. Finally, sections

were mounted on subbed glass slides, dehydrated, and cleared with xylene before being coverslipped. Fos-positive control tissue was used to confirm Fos-ir, and consisted of tissue from a male hamster that was exposed to female hamster vaginal secretions, which induces robust Fos-ir. Controls excluding primary and secondary antibodies were run using experimental tissue that did not contain the AVPV, with minimal nonspecific background staining.

**Radioimmunoassay for LH**

To determine the concentration of LH in blood samples from female rats, radioimmunoassay (RIA) for LH was performed. Plasma [LH] was determined from duplicate 50 µl samples using Rat LH RIA kit from A.F. Parlow, (Scientific Director, National Hormone and Peptide Program. Harbor-UCLA Medical center, Torrance, CA). The kit contained: anti-rat LH primary antibody (S11; used at a 1:30,000 dilution in normal rabbit serum-EDTA-PBS), rat LH (NIDDK-rLH-I; lot# AFP-12066B) used to iodinate, and rat LH reference prep (NIDDK-rLH-RP-3; lot# AFP-7187B) used to make standards. Secondary antibody (also from Parlow) was Goat Anti-Rabbit gamma globulin (GARGG) (Lot # 6/81; used at a 1:5 dilution in gel PBS). $I^{125}$ for iodination was purchased from Perkin Elmer (NEZ033A002MC). LH was iodinated according to previously published methods (Sisk and Desjardins, 1986), and was purified using a concanavalin A-Sepharose (Pharmacia, Piscataway, NJ) affinity chromatography column. Iodinated LH was displaced with 100 mM methyl a-n-mannopyranoside (Sigma). Sample concentrations are expressed as ng/ml, based on standard curve ranging from 0.8 ng/ml to 30 ng/ml. The lower limit of detectability for the assay was 0.8 ng/ml and all values that fell below

the assay sensitivity were adjusted to 0.8 ng/ml. Intraassay coefficient was 11.0%. Samples from this assay that were above the upper limit of detection, i.e. >30 ng/ml, were re-run with either 10 µl or 25 µl plasma samples, with standard curves ranging from 1.6 ng/ml-60 ng/ml or 4 ng/ml-150 ng/ml, respectively, with an intraassay coefficient of 6.6%.

**Microscopic Analyses and Quantification of Fos-ir**

To analyze the density of Fos (total number of Fos-ir cells/ $mm^2$) in the AVPV of female rats, 4 anatomically matched sections of the AVPV were selected from a 1-in-4 series. Analyses were performed on an Olympus BX51 microscope with brightfield illumination using Neurolucida software (MBF Bioscience; Williston, Vermont). The AVPV was located and traced bilaterally using adjacent Nissl-stained sections at 100x magnification, and traces were superimposed onto Fos-ir tissue sections. Fos-ir cells were counted at 400x magnification using an UPlanSApo 40x (0.9 NA) objective. Minimal contrast adjustments were made to the images, but images were otherwise unaltered.

**Statistical Analyses**

To determine if the Fos density in 4 anatomically matched sections of the AVPV was different in animals treated with oil or hormones, a one-way ANOVA was done with treatment (oil, hormone) as the independent variable and Fos density (# Fos-ir cells/$mm^2$) in the AVPV as the dependent variable (n = 2 oil-treated/ 4 hormone-treated).

***Experiment 2: To determine if pubertally born cells in the AVPV are involved in the LH surge***

**Animals and Experimental Design**

Sixteen weanling (P21) Sprague-Dawley female rats were ordered from Harlan and singly housed in 37.5 x 33 x 17 cm clear polycarbonate cages with *ad libitum* access to food (Teklad Rodent diet no. 8640; Harlan, Madison, WI) and water. Animals were maintained on a 14:10 light:dark cycle (lights off at 1600h). Animals were given a week to acclimate after arrival. During this time, they were handled daily. A week after arrival, animals underwent stereotaxic surgery to receive osmotic minipumps containing BrdU connected to intracerebroventricular (ICV) cannulas (see below). At the end of the 4-week administration of ICV BrdU, all females were ovariectomized (on P56). A week later, rats were given EB and P to induce a surge of LH and were perfused approximately 6 hours after P injection (same as above, in experiment 1, except P injection took place at 1000 h). See Figure 2.1.

Animals were treated in accordance with the National Institutes of Health's Guide for the Care and Use of Laboratory Animals. Michigan State University's Institutional Animal Care and Use Committee approved all protocols.

**ICV cannulation/osmotic minipump implantation**

A week after arrival, on P28-29, female rats underwent stereotaxic surgery and received ICV (1.00 mm posterior, 1.2 mm lateral, and-4.00 mm ventral from bregma) cannulas (Alzet Brain Infusion Kit 2) attached to minipumps (Alzet model #1004) containing 5-bromo-2'-deoxyuridine (BrdU; Sigma; 4.5 µg/µl) in sterile artificial cerebrospinal fluid (Harvard Apparatus, AH 59-7316). This particular pump model delivers solutions at 0.11 µl/hr for 28 days.

**Perfusions and sectioning**

Animals were perfused and the brains were section in the exact same fashion as above, in experiment 1.

**Double-label BrdU/Fos immunofluorescence**

To determine if pubertally born cells were active at the time of the LH surge, double-label immunofluorescence for BrdU and Fos was performed. The methods were performed as previously described (Mohr and Sisk, 2013), with minor changes. Tissue was rinsed with 0.05 M tris-buffered saline (TBS) in between all steps, and all incubations took place at room temperature, unless otherwise noted. A 1-in-4 series of free-floating sections were incubated in 0.1% sodium borohydride for 10 min to reduce autofluorescence. Sections were incubated in 2N HCL for 30 min at 37°C followed by a 10 min incubation in 0.1M borate buffer (pH = 8.5). Tissue was blocked for 1 hr in blocking solution containing 1% Triton-X-100, 1% bovine serum albumin, 1% hydrogen peroxide, and 20% goat serum in TBS, followed by a 48 h incubation at 4°C in a primary antibody cocktail solution containing monoclonal rat anti-BrdU (Serotec, MCA2060; 1:1000 dilution, working concentration 1 µg/ml) and polyclonal rabbit anti-c-Fos (Santa Cruz, sc-52; 1:10000 dilution, working concentration 0.02 µg/ml) in TBS-plus (0.3% triton-X 100 and 2% goat serum in TBS). After rinsing for 30 min in 0.3% triton-X 100 in TBS, sections were incubated for 2 h in a secondary antibody cocktail solution containing biotin-SP-conjugated AffiniPure goat anti-rat (Jackson, 112 065 003; 1:1000 dilution, working concentration 1.3 µg/ml) and Cy3-conjugated AffiniPure Goat anti-rabbit (Jackson, 111 165 144; 1:1000 dilution, working concentration 1.5 µg/ml). The BrdU label was detected with 1 h incubation in Cy2-conjugated streptavidin (Jackson, 016 220 084; 1:1000 dilution, working

concentration 1.8 µg/ml) and then sections were mounted onto glass slides and coverslipped using SlowFade gold antifade reagent (Life Technologies, S36936). BrdU-positive control tissue was used to confirm BrdU-ir, and consisted of tissue from a rat that got BrdU exposure during the latter end of gestation. Controls excluding primary and secondary antibodies were run using experimental tissue that did not contain the AVPV, with minimal nonspecific background staining.

**Double-label BrdU/ERα Immunofluorescence**

To determine if pubertally born cells in the AVPV express estrogen receptor alpha (ERα), sequential double-label immunofluorescence for BrdU and ERα was performed. Because estradiol down-regulates ERα immunoreactive labeling in the preoptic area (Caba et al., 2003), labeling was performed on tissue from animals that were ovariectomized and given oil approximately 6 hours before perfusion (oil-treated controls). Tissue was rinsed with 0.05M TBS in between all steps, and all incubations took place at room temperature, unless otherwise noted. A 1-in-4 series of free-floating sections were incubated in 0.1 % sodium borohydride for 10 minutes to reduce autofluorescence. Tissue was then blocked in 1 % hydrogen peroxide, 20 % normal goat serum, and 1 % bovine serum albumin in TBS for 1 hour, followed by incubation in rabbit anti-ERα primary antibody (Millipore, C1355; 1:25,000 dilution; 0.04 µg/ml working concentration) for 48 hours at 4°C. Following rinses in TBS + 0.3 % triton-x-100, tissue was incubated in biotinylated goat-anti-rabbit IgG (Vector, BA-1000; 1:1000 dilution, 1.5 µg/ml working concentration) for 1 hour, then rinsed again in TBS + 0.3 % triton-x-100. Tissue was incubated for 1 hour in avidin/ biotinylated enzyme complex reagent (ABC Elite Kit; Vector Laboratories), rinsed in TBS + 0.3 % triton-x-100, then incubated in biotinyl tyramide (1:500

dilution with 1x amplification buffer from TSA Biotin System kit, Perkin Elmer, NEL700A001KT). ERα signal was detected with Cy3-conjugated streptavidin (Jackson, 016-160-084; 1:500 dilution, 3 μg/ml working concentration) for 1 hour. Tissue was then labeled for BrdU. After a 30-minute incubation in 2 N HCl at 37°C, tissue was rinsed in borate buffer (pH 8.5) for 10 minutes, then incubated with BrdU monoclonal rat anti-BrdU (Serotec, MCA2060; 1:1000 dilution, 1 μg/ml working concentration) for 48 hours at 4°C. After rinses in TBS + 0.3 % triton-x-100, tissue was incubated in Cy2-conjugated goat anti-rat IgG (Jackson, 112-225-167; 1:1000 dilution, 1.5 μg/ml working concentration) for 1 hour. Tissue was mounted onto glass slides and coverslipped using SlowFade Gold antifade reagent (Life Technologies, S36936). BrdU-positive control tissue was used to confirm BrdU-ir, and consisted of tissue from a 1.5-2 month old rat whose dam received BrdU during the latter end of gestation. Controls excluding primary and secondary antibodies were run using experimental tissue that did not contain the AVPV, with minimal nonspecific background staining.

**Double-label BrdU/PR Immunofluorescence**

To determine if pubertally born cells in the AVPV express progesterone receptor (PR), double-label immunofluorescence for BrdU and PR was performed. Because estradiol up-regulates PR immunoreactive labeling in the preoptic area (Simerly et al., 1996), labeling was performed on tissue from animals that were ovariectomized and given estradiol benzoate then progesterone before perfusion (hormone-treated). A 1-in-4 series of free-floating sections were sequentially processed for PR and BrdU. The procedures were performed exactly as above for BrdU/ERα, except the primary antibody was rabbit polyclonal antibody against human PR (Dako, A009801-1; 1:1000 dilution, 1.2 μg/ml working concentration) and incubation in this

primary lasted 72 hours at 4°C. BrdU-positive control tissue was used to confirm BrdU-ir, and consisted of tissue from a rat that got BrdU exposure during the latter end of gestation. Controls excluding primary and secondary antibodies were run using experimental tissue that did not contain the AVPV, with minimal nonspecific background staining.

**Microscopic analysis and quantification**

BrdU/Fos, BrdU/ERα, and BrdU/PR colocalization were quantified in 4 anatomically matched sections of AVPV from female rats treated with ICV BrdU during puberty. Z stacks containing BrdU-ir cells in the AVPV were taken with an Olympus BX51 microscope under epi-illumination using MBF Bioscience's Image Stack Module for Neurolucida. Stacks were taken at 0.5-micron steps spanning the Z-axis of the cell using an UPlanSApo 40× (0.9 NA) objective. FITC filters were used to visualize BrdU-positive cells and TRITC filters were used to visualize Fos-, ERα-, or PR-positive cells. Red fluorescence was pseudo-colored magenta. Colocalization was confirmed using the 3D Visualization, and Neurolucida software was used for quantification of cells. Minimal contrast adjustments were made to the images, but images were otherwise unaltered.

**Statistical analyses**

To determine if the percent of BrdU-ir cells that colocalize with Fos-ir in the AVPV differs between oil and hormone-treatment, a one-way ANOVA was done with treatment (oil, hormone) as the independent variable and percentage of BrdU-ir cells that colocalized with Fos-ir as the dependent variable. (n = 6 oil-treated/ 7 hormone-treated).

***Experiment 3: To determine if cell addition during puberty is required for the ability to generate an LH surge***

**Animals**

Sixteen weanling (P21) and 16 adult (P58-65) female Sprague-Dawley rats) were ordered from Harlan and singly housed in 37.5 x 33 x 17 cm clear polycarbonate cages with *ad libitum* access to food (Teklad Rodent diet no. 8640; Harlan, Madison, WI) and water. Animals were maintained on a 14:10 light:dark cycle (lights off at 1600 h). Animals were treated in accordance with the National Institutes of Health's Guide for the Care and Use of Laboratory Animals. Michigan State University's Institutional Animal Care and Use Committee approved all protocols.

**Design**

Animals were ordered to arrive in 3 cohorts, with each cohort consisting of 4-6 P21 rats and 4-6 P58-65 rats. Results from the first LH radioimmunoassay (RIA), performed after the first cohort, instigated a slight change in experimental design of cohort 3. In all cohorts, the overall health of animals being treated with AraC was monitored, and no changes in body weight or general well-being were observed. See Figure 2.2.

Many problems occurred within the first cohort, causing the LH data from that cohort to be thrown out. First, catheter patency was an issue, leaving n = 1/age in control-treated, and 2/age/ in AraC-treated rats. In the only adult control, the hormone injections did not elicit LH secretion, and notes indicated that the injections leaked (i.e. oil was noted on her back). Therefore, there was no adult control. Second, experimental error caused blood samples to be

diluted. Specifically, the syringe was not changed when the lock solution was drawn out of the catheter, thus the blood samples contained both lock solution (heparinized saline) and blood. Because the samples were merely diluted, a surge was present in the Pubertal AraC animals and Pubertal control, as well as in the AraC-treated adults. In Pubertal-AraC animals, it appeared that the surge was delayed, but there was only 1 control animal to compare it to. Because it appeared that AraC-treated animals in the first cohort were able to generate an LH surge, we decided to probe for a surge of LH immediately after puberty, instead of waiting a couple weeks after puberty. We reasoned that the amount of time in between the end of AraC treatment and the induction of the LH surge was enough to add more cells to the AVPV that contribute to the LH surge.

Cohorts 1&2 design

Half of the animals received AraC ICV for 4 weeks, either during puberty (n = 5; Pubertal AraC) or in adulthood (n = 5; Adult AraC). The other half of the animals received only BrdU ICV for 4 weeks, either during puberty (n = 5; Pubertal Control) or in adulthood (n = 5; Adult Control) or. From this point forward, any method performed on Pubertal AraC or Adult AraC animals was also performed on the age-matched control animals. Vaginal opening, a peripheral indicator of the start of puberty, was monitored in the Pubertal AraC group. On P69-70 (Pubertal AraC) and P106-114 (Adult AraC), rats were ovariectomized. To minimize the number of times the animals underwent anesthesia (isoflurane), at the same time as ovariectomy animals received a femoral vein catheter (Alzet, custom-made rat femoral catheter) used for repeated blood sampling. Animals were allowed to recover for 2 days, and then an LH surge was induced (same methods as experiment 1, except P injection took place at 1000 h, see

above). In cohort 1, on P74 (Pubertal AraC) and P111-118 (Adult AraC) starting at 0800h, blood samples (200 µl) were taken hourly until 1240h, then every 20 minutes from 1240h-1620h (during the time of the expected LH surge), then hourly from 1700h-2400h. On P78 (Pubertal AraC), and P115-122 (Adult AraC) animals were perfused at 1600h. Blood sampling for cohort 2 occurred at the same times as in cohort 3 (see below). See Figure 2.2.

Cohort 3 design

Half of the animals received AraC ICV for 4 weeks, either in adulthood (n = 3; Adult AraC) or during puberty (n = 2; Pubertal AraC). Age-matched controls received just ICV vehicle solution (BrdU in aCSF) via osmotic minipump (n = 3/ age). On P54-55 (Pubertal AraC) and P91-99 (Adult AraC) rats were put under using isoflurane anesthesia, were ovariectomized and received a femoral vein catheter. Animals were allowed to recover for 2 days, and then an LH surge was induced (same methods as experiment 1, except P injection took place at 1000 h, see above). On P59 (Pubertal AraC) and P96-103 (Adult AraC) blood samples (200 µl) were taken hourly from 1100h until 1300h, then every half-hour from 1350-1500h, and hourly from 1500h-1900h. A few days later another LH surge was induced, and animals were perfused at the expected time of the surge, on P65 (Pubertal AraC) and P101-108 (Adult AraC). See Figure 2.2.

**ICV cannulation/osmotic minipump implantation**

Animals were given a week to acclimate after arrival. During this time, they were handled daily. On P28/ P65-72 rats received ICV (1.00 mm posterior, 1.2 mm lateral, and-4.00 mm ventral from bregma) cannulas (Alzet Brain Infusion Kit 2) attached to minipumps (Alzet model #1004) containing cytosine arabinoside hydrochloride (AraC; Sigma; 33 µg/µl) with

vehicle (experimental groups) or vehicle solution alone (control groups). The vehicle solution contained sterile artificial cerebrospinal fluid and 5-bromo-2'-deoxyuridine (BrdU; Sigma; 4.5 μg/μl). This particular model minipump delivers solution for up to 4 weeks.

**Perfusions and sectioning**

Animals were perfused and the brains were section in the exact same fashion as above, in experiment 1.

**Single-label BrdU immunohistochemistry**

To determine efficacy of AraC treatment, single-label immunohistochemistry was performed. A 1-in-4 series of free-floating sections were rinsed in Tris-buffered saline (TBS; 0.05 M). Endogenous peroxidase activity was eliminated by incubation in 0.6% $H_2O_2$ for 30 min. Sections were placed in 2 N HCl for 30 min at 37 °C, and then rinsed for 10 min in borate buffer (0.1 M; pH 8.5). The tissue was blocked in AffiniPure Fab Fragment donkey anti-rat IgG (Jackson ImmunoResearch, cat no. 712-007-003, working concentration 12 μg/ml) in TBS with 0.1% triton-x-100 and 3% donkey serum (Jackson ImmunoResearch), then incubated overnight at 4 °C in monoclonal primary antibody rat anti-BrdU (Serotec, MCA2060; 1:1000 dilution, at a working concentration of 1 μg/mL). Sections were incubated for 2 h in Biotin-SP-conjugated AffiniPure donkey anti-rat secondary antibody (Jackson ImmunoResearch, 712–065-150; 1:1000 dilution, at a working concentration of 2 μg/mL), then for 60 min with avidin/ biotinylated enzyme complex reagent (ABC Elite Kit; Vector Laboratories), and reacted with 3,3'-diaminobenzidine tetrahydrochloride (Sigma-Aldrich, catalog no. D5905; 0.25mg/ml) with 0.012% hydrogen peroxide in 0.05 TBS for 2.75 min. Sections were thoroughly rinsed in TBS

before and between all incubations. Unless otherwise noted, incubations and washes occurred at room temperature. Finally, sections were mounted, dehydrated, and cleared with xylene before being coverslipped. BrdU-positive control tissue was used to confirm BrdU-ir, and consisted of tissue from a 1.5-2 month old rat whose dam received BrdU during the latter end of gestation. Controls excluding primary and secondary antibodies were run using experimental tissue that did not contain the AVPV, with minimal nonspecific background staining.

**Double-label BrdU/Fos Immunofluorescence**

To determine if there are differences in the proportion of pubertal- vs. adult-born cells in the AVPV that are active during a hormone-induced LH surge in adulthood, double-label BrdU/Fos immunofluorescence was performed on tissue from control animals (that just received BrdU). The procedures were performed exactly as above, in experiment 2.

**Triple-label BrdU/GFAP/NeuN Immunofluorescence**

To determine if AraC treatment alters the proportion of cellular phenotype (i.e. the percentage of BrdU-ir cells expressing GFAP or NeuN) triple labeling with BrdU, astrocyte marker glial fibrillary acidic protein (GFAP), and mature neuronal nuclei marker (NeuN) was performed. The methods were completed as previously described (Mohr and Sisk, 2013), with minor changes. A 1-in-4 series of free-floating sections were incubated in 0.1% sodium borohydride for 10 minutes to reduce autofluorescence. Sections were incubated in 0.93N HCL for 30 minutes at 37°C followed by a 10-minute incubation in 0.1M borate buffer. Tissue was blocked for 1 hour in TBS-plus (0.3% Triton-X-100 and 6% goat serum in TBS), followed by a 48

hour incubation at 4°C in a primary antibody cocktail solution containing monoclonal rat anti-BrdU (Serotec, cat no. MCA2060; 1:1000 dilution, working concentration 1 µg/ml), monoclonal mouse anti-NeuN (Chemicon, cat no. MAB377, clone A60; 1:1000 dilution, working concentration 1 µg/ml), and polyclonal rabbit anti-GFAP (Dako, cat no. Z0334; 1:5000 dilution, working concentration 0.58 µg/ml) in TBS-plus. Sections were incubated for 2 hours in a secondary antibody cocktail solution containing biotin-SP-conjugated AffiPure goat anti-rat (Jackson, cat no. 112 065 003; 1:1000 dilution, working concentration 1.3 µg/ml), Cy3-conjugated AffiniPure Goat anti-rabbit (Jackson, cat no. 111 165 144; 1:500 dilution, working concentration 3 µg/ml) and Alexa Fluor 635 goat anti-mouse (Life Technologies, cat no. A-31574; 1:500 dilution, working concentration 4 µg/ml). The BrdU label was detected with a 1 hr incubation in Cy2-conjugated streptavidin (Jackson, cat no. 016 220 084; 1:1000 dilution, working concentration 1.8 µg/ml) and then sections were mounted onto glass slides and coverslipped using SlowFade gold antifade reagent (Life Technologies, cat no. S36936). BrdU-positive control tissue was used to confirm BrdU-ir, and consisted of tissue from a 1.5-2 month old rat whose dam received BrdU during the latter end of gestation. Controls excluding primary and secondary antibodies were run using experimental tissue that did not contain the AVPV, with minimal nonspecific background staining.

**Radioimmunoassay for LH**

To determine if AraC treatment during puberty or during adulthood affected the ability to generate an LH surge following hormone priming, RIA for LH was performed on blood samples taken during the time of the expected surge, with exactly the same methods as above, in experiment 1.

**Microscopic analyses and quantification**

Single-label BrdU

To determine the effectiveness of AraC treatment, the total numbers of BrdU-ir cells were counted in 4 anatomically matched sections of the AVPV from female rats treated with AraC or vehicle. Because the vehicle solution contains BrdU, the total number of BrdU-ir cells signifies both the level of cytogenesis in control (vehicle-treated) animals during puberty or during adulthood, and how effective AraC is at inhibiting cytogenesis in animals treated with AraC during puberty or during adulthood. Procedures for quantifying BrdU-ir cells in the AVPV are the same as above for quantification of Fos-ir cells in the AVPV (experiment 1).

Double-label BrdU/Fos

To determine how many pubertally or adult-born cells are active in the AVPV during the LH surge, BrdU/Fos colocalization was quantified in 4 anatomically matched sections from control animals treated with ICV BrdU during puberty or adulthood (n = 3/age). Procedures for acquiring image stacks and quantification are the same as above for quantification of BrdU/Fos in experiment 2.

Triple-label BrdU/GFAP/NeuN

To determine if cells born during puberty or adulthood differentiate into astrocytes or neurons, as well as to determine if AraC treatment alters these phenotypes, BrdU/GFAP or BrdU/NeuN colocalization was quantified in 4 anatomically matched sections of the AVPV in AraC- or vehicle-treated animals (n = 2/age/treatment). Z stacks containing BrdU-ir cells in the AVPV were taken with an Olympus BX51 microscope under epi-illumination using MBF

Bioscience's Image Stack Module for Neurolucida. Stacks were taken at 0.5-micron steps spanning the Z-axis of the cell using an UPlanSApo 40× (0.9 NA) objective. FITC, TRITC, and near-IR filters were used to visualize BrdU-, GFAP-, and NeuN-positive cells, respectively. Colocalization was confirmed using the 3D Visualization, and Neurolucida software was used for quantification of cells. Red fluorescence was pseudo-colored magenta. Minimal contrast adjustments were made to the images, but images were otherwise unaltered.

**Statistical Analyses**

Plasma LH data

To determine if AraC treatment blunted the LH surge, t-tests were performed at each time point to determine if plasma LH concentration differed between AraC-treated and control animals, and were performed separately for each age during treatment (i.e. puberty and adulthood). Hedges g, a calculation of effect size that corrects for small sample size was also computed to provide standardized effect sizes of mean differences between AraC treated and age-matched controls in [LH]. These calculations were performed in the same manner as the t-tests, above.

To determine whether the size of the LH surge differed between animals treated with AraC during puberty or adulthood compared to age-matched controls, Area Under Curve calculations were performed.

Within each animal, the peak value of plasma LH was noted along with the time the peak occurred. ANOVAs were done to determine if AraC treatment affected mean maximum [LH] or the mean timing of the LH peak.

Maximum [LH] vs. Total BrdU in AVPV

To understand the relationship between mean maximum plasma LH and the total number of BrdU-ir cells in 4 anatomically matched sections of the AVPV, a linear regression was performed.

Single-label BrdU

To determine if the effectiveness of AraC differed when given during puberty or adulthood, two-way ANOVA was done with age during treatment (puberty or adulthood) and treatment (AraC or vehicle) as the independent variables and the total number of BrdU-ir cells in 4 anatomically matched sections of the AVPV as the dependent variable (n = 7 pubertal control; 5 pubertal AraC; 6 adult control; 7 adult AraC).

BrdU/GFAP/NeuN

To determine if the percentage of cells displaying a particular phenotype differed between groups (Pubertal control, Pubertal AraC, Adult control, and Adult AraC) or between phenotypes (BrdU only, BrdU/GFAP, and BrdU/NeuN), ANOVA was performed, n =2/age/trt.

BrdU/Fos

To determine if there were differences in the percentage of pubertally vs. adult-born cells in the AVPV that were active during the LH surge, ANOVA was performed with the percentage BrdU-ir cells expressing Fos as the dependent variable and age during BrdU treatment as the independent variable (puberty vs. adulthood).

## RESULTS

### *Female rats show a surge of LH 4 hrs after P injection, and Fos corresponding to the LH surge approximately 6 hours after P injection- experiment 1*

Ovariectomized female rats exhibited a surge of LH that occurred approximately 4 hours following P injection (which had been preceded by two days of EB injections; Figure 2.3). The peak [LH] was 35.14 ± 8.67 ng/ml, which occurred at 1500 h. Area under curve calculations, which can be used to measure the size of the LH surge, was 12,627 ng/ml/hr.

Mean Fos-ir density in the AVPV was 267 ± 54 in hormone-treated and 75 ± 47 in oil-treated female rats, ~6 hours after P injection. No statistically significant differences in Fos-ir between hormone and oil-treated rats were observed, likely due to small sample sizes and one animal not having much Fos-ir in the AVPV after hormone-priming. However, Hedges' g, a measure of effect size that corrects for small sample sizes, is large (1.5) when comparing Fos-ir cells in hormone vs. oil-treatment (Figure 2.4).

### *Pubertally born cells in the AVPV express Fos during a hormone-induced LH surge-experiment 2*

After priming OVX female rats with EB and P, 31.8 ± 2.8% of BrdU-ir cells in the AVPV express Fos-ir during the time of the expected LH surge, while after oil treatment, only 8.4 ± 2.6% of BrdU-ir cells in the AVPV express Fos. ANOVA determined that the percentage of BrdU-ir cells in the AVPV that express Fos-ir differs with hormone or oil treatment (Figure 2.4, $F(1,11) = 35.676$, $p \leq 0.0001$). Thus, hormone-induction of the LH surge results in a 378% increase in the percentage of pubertally born cells that are active in the AVPV.

***Some pubertally born cells in the AVPV express ER, but none express PR- experiment 2***

Immunofluorescent labeling of BrdU with ERα revealed that about 9 ± 1% of BrdU-ir cells in the AVPV of oil-treated OVX female rats express ERα (Figure 2.6). Additionally, another 6 ± 1% of BrdU-ir cells expressed ERα labeling that was not nuclear, but punctate and appeared to be membrane ERα. No BrdU-ir cells expressed PR in the AVPV of hormone-primed OVX female rats.

***AraC treatment starting at P28 does not alter vaginal opening-experiment 3***

Day of vaginal opening, a peripheral indicator of the start of puberty in female rats, did not differ between animals treated with ICV AraC or vehicle solution during puberty ($p > 0.3$).

***AraC treatment during puberty or during adulthood reduces and delays the LH surge-experiment 3***

Animals treated with AraC during puberty or for an equal amount of time during adulthood that were probed for a LH surge 2-3 weeks after the end of AraC treatment displayed a LH surge that was blunted and delayed, compared to age-matched controls (see figure 2.7). While t-tests found no statistically significant differences between animals treated with AraC during puberty compared to age-matched control animals in [LH] across time (Figure 2.7a), effect sizes were large during the time of the surge (i.e. Hedges' g, a calculation of effect size that corrects for small sample size, was 1.2, 1.6, and 1.1 at 1200, 1300, and 1350 respectively), see table 1. T-tests comparing [LH] in animals treated with AraC during adulthood to age-matched controls found that at 1350 and 1450 h there were statistically significant differences ($p$'s < 0.01; see figure 2.7b). Furthermore, Hedges' g effect sizes were large from 1350 h to 1600

h (1.3, 1.2, 1.2, 1.3, and 1.0, for 1350, 1400, 1450, 1500, and 1600 h, respectively), indicating that AraC treatment during adulthood reduced [LH] during the surge. Area Under Curve calculations on Figs 2.7a and b revealed that AraC treatment during puberty or during adulthood reduced the LH surge by 17% and 21%, respectively (Figure 2.7c).

AraC treatment reduced mean maximum [LH] (Figure 2.7d). ANOVA found a main effect of treatment on mean maximum [LH], where AraC-treated animals had a lower maximum [LH] compared to control animals ($F(1,11) = 7.080$, $p = 0.022$). Furthermore, ANOVA revealed that the mean timing of LH peak was delayed in AraC-treated animals (Figure 2.7e; $F(1,11) = 4.412$, $p = 0.06$).

***More cell addition in the AVPV is associated with higher concentration of LH in the blood following hormone-priming-experiment 3***

A regression analysis in which maximum [LH] was predicted from the linear effect of total number of BrdU-ir cells in the AVPV was conducted, and revealed a linear trend between the two variables, $F(1,12) = 4.363$, $p = 0.058$, $\beta = 0.516$, $b = 0.06$, $R^2 = .267$ (Figure 2.8). Thus, each additional BrdU-ir cell in the AVPV is associated with a 0.06 ng/ml increase in maximum [LH].

***ICV AraC treatment reduces the number of BrdU-ir cells in the AVPV and more cells are added to the AVPV during puberty than during adulthood-experiment 3***

ANOVA using the mean # of BrdU-ir cells in the AVPV of 4 anatomically matched sections as the dependent variable and treatment (AraC or vehicle) and age during treatment (puberty or adult) as independent variables was done to determine if the mean # of BrdU cells

in the AVPV differed between animals treated with AraC or vehicle, in puberty or in adulthood (Figure 2.9). Main effects of treatment and age during treatment were found. That is, AraC ICV reduced the mean number of BrdU-ir cells in the AVPV by 58% ($F(1,21) = 16.648$, $p \leq 0.001$), and there were 41% more BrdU-ir cells in animals treated with BrdU during puberty than during adulthood ($F(1,21) = 6.687$, $p = 0.017$). Thus, cell addition is higher in the AVPV during puberty than during adulthood.

***AraC treatment increases the percentage of pubertally or adult-born cells that differentiate into astrocytes-experiment 3***

ANOVA was performed to determine if the percentage of cells displaying a particular phenotype differed between groups (Pubertal control, Pubertal AraC, Adult control, and Adult AraC) or between phenotypes (BrdU only, BrdU/GFAP, and BrdU/NeuN; see Figure 2.10). A main effect of phenotype ($F(2, 2) = 73.00$, $p = 0.0135$) was qualified by a significant phenotype-by-group interaction ($F(6, 6) = 7.031$, $p = 0.0159$), where animals treated with AraC during puberty had a higher percentage of astrocytes (mean = 51.56%) compared to animals treated with AraC during adulthood (mean = 30.42%), or animals treated with vehicle during adulthood (Adult control; mean = 28.11%). Additionally, animals treated with AraC during adulthood had significantly more BrdU-ir only cells compared to animals treated with AraC during puberty (67.58% vs. 42.97%, respectively).

The animals (n = 2/age/trt) chosen for phenotypic analyses were randomly selected, thus the average total BrdU in Adult control animals (mean = 164) appears higher than the average total BrdU for Pubertal control animals (mean = 105), which is not the case when looking at the total number of single-label BrdU-ir cells. One adult control animal had a total of

195 BrdU-ir cells, whereas one pubertal control had only 69 BrdU-ir cells. Importantly, the standard deviations in the control animals were low, therefore, even though the actual numbers of BrdU-ir cells varied between animals, the percentage of those cells expressing NeuN or GFAP remained relatively stable. It should also be noted that many more cells are BrdU-ir when single-label immunohistochemistry is done compared to triple-label immunofluorescence and could be due to photobleaching or variations in labeling techniques. Hence, all data using immunofluorescence techniques are expressed as percentages.

***About half of pubertally and adult-born cells express Fos during a hormone-induced LH surge-experiment 3***

While there were no significant differences in the percentage BrdU-ir cells expressing Fos between animals treated with BrdU during puberty or adulthood, 50% of pubertally born and 54% of adult-born cells express Fos during the expected time of a hormone-induced LH surge.

## DISCUSSION

The preovulatory LH surge in female rats is coordinated by the AVPV, as it integrates hormonal and circadian signals to generate and time the GnRH/LH surge. The induction of the LH surge in female rats normally involves a positive-feedback response to estradiol and progesterone and it can only be elicited after puberty. Because the LH surge cannot be elicited before puberty in female rats, we hypothesized that the cellular machinery responsible for regulation of the LH surge is not yet in place. Here, we demonstrate that neurons and astrocytes are added to the female rat AVPV after puberty, and that these new cells become

integrated into a circuit that controls the preovulatory surge of LH. We suggest cell addition in the AVPV as a mechanism to maintain HPG axis function in female rats.

***Cells added to the AVPV after puberty are active during a hormone-induced LH surge***

Almost half of cells born during puberty (P28-56) or during early adulthood (P65-100) expressed Fos during a hormone-induced LH surge, indicating that cells added to the AVPV after puberty are functionally integrated into hormonally sensitive neural circuits that participate in the preovulatory LH surge. In experiment 2, hormone treatment caused a 378% increase in the activation of pubertally born cells in the AVPV during the LH surge (i.e. 30% BrdU/Fos in hormone-treated vs. 9% BrdU/Fos in oil-treated), demonstrating that newly born cells in the rat AVPV are responsive to steroid hormones. In experiment 3, ~50% of cells born during puberty or adulthood were active during a hormone-induced LH surge.

The amount of Fos expression in newborn cells in the female rat AVPV is higher than what was previously reported in male hamsters after mating, indicating that a larger proportion of the population of newborn cells in the female rat AVPV are active during a hormonally induced LH surge (30 - 50%) compared to the amount of pubertally born cells that are active during mating in the male hamster medial preoptic area, dentate gyrus, medial amygdala, and arcuate nucleus (~3%)(Mohr and Sisk, 2013). The experimental designs between the current and the former study are very similar, with BrdU treatment throughout puberty and perfusions occurring ~1 month after the end of BrdU treatment. The higher level of activation of newborn cells in the female rat AVPV compared to pubertally born cells in the male hamster more likely reflects that there is a higher recruitment of newborn cells in the control of the hormonally mediated GnRH/LH surge compared to the amount of pubertally born cells that are active

during mating. Moreover, the hamsters used in the mating experience were sexually naïve, and perhaps there would be a higher degree of activation in pubertally born cells had the hamsters been sexually experienced. In the current study, the female rats were ovariectomized about 1 month after vaginal opening, thus the newborn cells in the AVPV possibly had a chance to participate in the LH surge before testing. Finally, although the Fos response to mating in the male hamster is very well characterized, there were no Fos controls (i.e. hamsters that were placed into an empty cage) (Mohr and Sisk, 2013). Fos expression in the AVPV is low but not entirely absent in the absence of hormone priming, so it is not surprising that some BrdU/Fos cells were observed in oil-treated rats. Hormone priming caused a 3.8 fold increase in the activation of pubertally born cells in the AVPV over just oil injections, proving that these cells are functionally integrated into a hormonally sensitive circuit. Together, these studies shed light on cells that are born during puberty that contribute to adult reproductive behavior and function.

The increase in activation of pubertally born cells from the second to the third experiment could be because the cells in the third experiment were 13 days older than the cells in the second experiment, thus having more time to differentiate and integrate into neural circuits. Peak immediate early gene (IEG) expression occurs in the dentate gyrus when BrdU cells are 3 weeks old, with 25% of them expressing zif268 after a hippocampus-dependent learning experience. Those active cells make up 50% of the population of cells that are active during a kainite-induced seizure, indicating that half of the functional population of newborn cells in the dentate gyrus (DG) are active during hippocampus-dependent learning (Snyder et al., 2009). Snyder and colleagues also examined IEG expression in the DG when BrdU cells were

10 weeks old and found that only 4% of the functional population of cells expressed zif268, suggesting a preferential activation of younger cells in the dentate gyrus (Snyder et al., 2009). Although a time course experiment was not done in the current study, it is likely that the cells born during BrdU treatment had just the right amount of time to differentiate and integrate into a hormonally sensitive circuit.

If Fos is a marker of *neuronal* activation, the finding that 30-50% of pubertally or adult-born cells in the AVPV express Fos during the LH surge is at odds with the present and earlier studies showing that between 10-15% of these newly born cells are likely mature neurons, indicated by NeuN staining when examined 3 weeks after the end of BrdU treatment (i.e. when BrdU cells were 3-7 weeks old). Several possibilities exist to explain the discrepancy between Fos and NeuN expression in newly born cells. First, not all mature neurons express NeuN. Neurons devoid of NeuN expression include: cerebellar Purkinje neurons, olfactory bulb mitral cells, retinal photoreceptor cells, Cajal-Retzius cells, neurons in the inferior olivary nucleus, dentate nucleus, sympathetic ganglia, cells in most of the inner nuclear layer, and some neurons within the suprachiasmatic nucleus (Mullen et al., 1992 1998, Morin, 2011, Duan, 2015). Not all neurons express NeuN in the suprachiasmatic nucleus (SCN), a brain structure that lies just caudal to the AVPV (Morin et al., 2011), and expression is variable amongst dopaminergic neurons in the substantia nigra (Cannon and Greenamyre, 2009). Neurons in the AVPV could also take longer to differentiate and express NeuN, as is the case for cells in particular subdivisions of the hippocampus (Snyder et al., 2012). Not only are some neuronal populations devoid of NeuN expression, the integrity of NeuN immunoreactivity has been called into question. NeuN immunoreactivity is diminished during certain physiological states or

diseases, for example, in the spinal cord during aging (Portiansky et al., 2006), and following axotomy (Unal-Cevik et al., 2004). Thus, there is likely a population of neurons in the AVPV that do not express NeuN, but could be expressing Fos in this study. Second, several *in vitro* and *in vivo* studies have shown that astrocytes are capable of expressing Fos (Hengerer et al., 1990; Hisanaga et al., 1990; Ladenheim et al.; Matsunaga et al., 2001; Tchelingerian et al., 1997; Yuan et al., 2010), including in the nearby suprachiasmatic nucleus (Bennett and Schwartz, 1994). Roughly a third of cells born to the AVPV after puberty are astrocytes, which in addition to neurons may also be expressing Fos during the LH surge.

Astrocytes in the AVPV play a crucial role in the GnRH/LH surge. Astrocytes help regulate GnRH release through classic mechanisms such as the release of growth factors (for reviews see (Dhandapani et al., 2003; Ojeda et al., 2010)) and by dynamically ensheathing neurons and processes, altering electrical and chemical transmission (Ullian et al., 2001). Astrocytes directly appose GnRH neurons, and the surface area and number of processes that appose GnRH neurons fluctuates in parallel with the fluctuations in plasma LH concentration (Cashion et al., 2003). Additionally, hypothalamic astrocytes rapidly synthesize neuroprogesterone through membrane ERα (mERα) signaling (Kuo et al., 2010c; Micevych et al., 2003a; Micevych and Sinchak, 2011; Sinchak et al., 2003). If neuroprogesterone synthesis is blocked, the estrogen-induced LH surge is also blocked (Micevych et al., 2003c). Approximately 6% of pubertally born cells in the current study looked as if they contained mERα, and these cells could be astrocytes that secrete neuroprogesterone. However, because mERα is difficult to confirm without techniques such as surface biotinylation (Kuo and Micevych, 2012), further work is needed to confirm the presence of mERα on pubertally born cells.

Approximately 10% of pubertally born cells in the AVPV expressed nuclear ERα. ERα signaling near the AVPV is required for the LH surge to occur (Wintermantel et al., 2006), and if ERα is deleted specifically within kisspeptin neurons, no surge occurs (Mayer et al., 2010). ERα is expressed by nearly 70% of kisspeptin neurons in the AVPV. Kisspeptin neuron number increases from P20 to adulthood in female mice in the AVPV, but not arcuate nucleus (Mayer et al., 2010). About 1/3 of kisspeptin neurons express Fos during a hormone-induced LH surge in mice (Clarkson et al., 2008), thus the BrdU/ERα positive cells in the current study could be kisspeptin neurons. Approximately 60% of kisspeptin neurons in the mouse AVPV express PR after hormone-priming (Clarkson et al., 2008), and no BrdU/PR colocalized cells were observed in the present study, suggesting that if the BrdU/ERα colocalized cells are kisspeptin neurons, then they are a part of the kisspeptin population devoid of PR. Kisspeptin immunoreactivity in the AVPV of rats is difficult to detect without inhibiting axonal transport (Overgaard et al., 2013), so more work is needed to determine if pubertally born cells in the AVPV are indeed kisspeptin neurons.

***Female rodent AVPV is a site of ongoing cell turnover, with a decline in cytogenesis in adults***

Newborn neurons and astrocytes were observed in the adult rat AVPV, demonstrating that cell turnover continues into adulthood. Cell addition is higher in the female rat AVPV during puberty, and between puberty and adulthood there is a 40% decrease in the addition of cells to the female rat AVPV. This decline in cytogenesis from puberty to adulthood is observed in other brain regions, such as the dentate gyrus of the hippocampus (He and Crews, 2007; Okamoto et al., 2012) the nucleus accumbens, and prefrontal cortex (Staffend et al., 2014), and emphasizes the plasticity of the pubertal brain. Even though there was a higher degree of cell

addition to the AVPV during puberty compared to adulthood, the patterns of differentiation were the same across age groups, i.e. the relative proportions of BrdU-ir cells expressing NeuN or GFAP did not differ between age groups. Thus, between 10-13% of cells added to the AVPV after puberty were neurons, whereas between 30-40% were astrocytes.

Earlier studies attempting to determine the phenotype of pubertally born cells in the rat AVPV found that over half of the BrdU-ir cells expressed NeuN and none expressed GFAP (Ahmed et al., 2008). Many methodological differences could account for this discrepancy. First, the duration and route of BrdU treatment was vastly different (i.e. 3 ip injections on P30-32 vs. 4 weeks of continuous ICV infusion). In the SVZ, there is a circadian gating of neurogenesis, such that expression of clock gene PERIOD2 temporally gates cell-cycle entry of neural progenitor cells and BMAL1 controls cell cycle entry and exit (Bouchard-Cannon et al., 2013). If there is a circadian gating of astrocytogenesis, animals getting central BrdU via osmotic minipump could conceivably have more newly born astrocytes than animals that just got BrdU ip once during the day. In other words, if there were a circadian window for astrocytogenesis (e.g. such that neural progenitor cells entered the cell cycle in the night) ICV infusion of BrdU would label newly born astrocytes whereas an IP injection in the middle of the day would not label newly born astrocytes. Central infusion of BrdU via osmotic minipump allows periventricular cytogenic zones continuous access to BrdU, whereas a peripheral injection gives the brain access to BrdU for only about 1- 2 h (Cifuentes et al., 2011). Second, the staining protocols were different, with the former study performing BrdU/NeuN and BrdU/GFAP double labeling, and the current study performing BrdU/GFAP/NeuN triple labeling with a different GFAP primary antibody. Third, the BrdU-ir cells in the former study were only 20-22 days old, whereas the BrdU-ir cells

in the current study were 3-7 weeks old, thus having more time to differentiate. Finally, the results from the former study were qualitative, whereas the relative neuronal or astrocytic phenotypes were quantified in the current study.

The ongoing addition of cells to the female rat AVPV could be driven by gonadal hormone secretion. Indeed, prepubertal gonadectomy decreases cell addition to the AVPV in female rats whereas it has no effect on cell addition to the AVPV in males (Ahmed et al., 2008), so at least a population of pubertally born cells in the female rat AVPV exists as a result of gonadal hormone secretion. Within the dentate gyrus, fluctuations in gonadal hormone secretion across the estrous cycle increase cell proliferation in females compared to males (Pawluski et al., 2009; Tanapat et al., 1999; Tanapat et al., 2005), such that 21 days after BrdU injection there is no difference between the number of cells that proliferated during proestrus and estrus (Tanapat et al., 1999). Within the amygdala, both TP and E increase BrdU labeling in castrated male meadow voles (Fowler et al., 2003; Fowler et al., 2005). In the dentate gyrus, amygdala, and ventromedial nucleus of the hypothalamus (VMH), between 43-89% of newly born BrdU-labeled cells (between 6 and 24 hours old) express ERα in the male meadow and prairie vole (Fowler et al., 2005), indicating that estrogen has the ability to act directly on newly proliferated cells or on progenitor cells. It remains to be elucidated whether gonadal hormone secretion throughout adulthood in females drives the ongoing addition of cells in the female rat AVPV, as it does in the pubertal rat AVPV.

Aside from gonadal hormones, growth factors such as insulin-like growth factor-1 (IGF-1) are also potent facilitators of cellular proliferation (for reviews see (Anderson et al., 2002; Llorens-Martin et al., 2009)). Of note, IGF-1 stimulates the birth of new neurons, astrocytes,

microglia, tanycytes, and endothelial cells within the periventricular zone of the hypothalamus (Perez-Martin et al., 2010). In previous studies we have identified pubertally born neurons, astrocytes, and microglia in the female rat AVPV (Chapter 1). Besides driving cytogenesis, IGF-1 plays a crucial role in the onset of puberty and regulation of GnRH release (for reviews see (Daftary and Gore, 2005; Garcia-Segura et al., 2008 2008)). Hypothalamic IGF-1 mRNA expression increases at the onset of reproductive function and decreases at reproductive senescence (Miller and Gore, 2001). Thus, because IGF-1 stimulates neuro- and gliogenesis the decrease in IGF-1 levels with age could account for the decrease in cytogenesis in the AVPV observed from puberty to adulthood. Given the decline in cytogenesis from puberty to adulthood, one could speculate that cytogenesis continues to decline in the female rat AVPV as reproductive senescence approaches. Whether the decline in cell addition with age contributes to reproductive senescence remains unknown, but prompts further investigation

If cells are added throughout life to the female rat AVPV, it is likely that cell addition, along with cell death, maintains the morphological sexual dimorphism in the rat AVPV. Indeed, there is a sex difference in the addition of pubertally born cells to the AVPV, where females have more newborn cells compared to males ((Ahmed et al., 2008); this document, Chapter 1). Cell death is crucial in maintaining sex differences in cell density and volume of the AVPV; overexpression of anti-apoptotic protein Bcl-2 (Zup et al., 2003) and deletion of pro-apoptotic protein Bax (Forger et al., 2004) eliminates the morphological sex difference in the AVPV. If cell death were the only mechanism that maintains these sex differences, there would be an age-related decline in AVPV volume, which is not the case in female rats (Chakraborty et al., 2003). While these results insinuate that cell addition is a mechanism for maintaining morphological

sex differences in the AVPV, studies comparing cell addition in adult male and female rats are needed to confirm this idea.

***Blocking cell addition after puberty reduces the LH surge***

Central knockdown of cell addition during puberty or for an equal amount of time during early adulthood delayed and blunted the LH surge in female rats, suggesting that newly born cells are involved in reproduction. In a previous study, we found that pubertally born cells in hypothalamic and limbic regions of male hamsters were active during mating in adulthood (Mohr and Sisk, 2013). Another study in male rats found that ICV treatment of AraC diminished mating behavior, causing lower intromission frequency, copulatory efficiency, and not a single rat ejaculated (Lau et al., 2011). While these authors concluded that newborn cells in the SVZ and hippocampus are important for reproduction, they overlooked the possibility that AraC was inhibiting cell addition to other regions of the brain, such as the hypothalamus or amygdala.

AraC treatment delayed the LH surge, suggesting that newly born cells help coordinate the precise timing of the preovulatory LH surge. The LH surge occurs only after the AVPV receives permissive circadian signals from the SCN, integrated with hormonal signals. No surge occurs if the SCN is lesioned (Wiegand et al., 1980). The AVPV itself displays oscillations in clock gene expression (Smarr et al., 2013), and these are thought to be the integrators of circadian signals from the SCN and ovarian hormonal signals to gate the timing of the LH surge. It could be that some newly born cells in the AVPV receive circadian input to help coordinate the timing of the LH surge, and blocking the addition of newly born cells interferes with this precise timing. In the present study, BrdU-ir cells were observed in the SCN, although not quantified, and because AraC was delivered centrally, newborn cells in the SCN itself could help coordinate the

timing of the LH surge. Because AraC treatment delayed the LH surge only by ~30 min, it seems unlikely that the circadian signal solely depends on newly born cells. Furthermore, blood sampling to determine the concentration of plasma LH was only carried out for 8 hours so it is unknown whether AraC treatment caused, for example, an additional LH surge in the night, or the following day. Nonetheless, more work is needed to determine the exact role of pubertally and adult-born cells in the timing of LH surge.

The knockdown of cell addition during puberty or adulthood diminished the surge of LH following hormone priming in female rats, indicating that pubertally and adult-born cells are involved in estrogen positive feedback. AraC treatment reduced the size of the LH surge by 17% and 21% compared to age-matched controls, depending on whether the treatment was during puberty or during adulthood, respectively. While it appears that AraC treatment during adulthood was more deleterious on the ability to generate an LH surge compared to AraC treatment during puberty, the effectiveness of AraC at inhibiting cell addition must be considered. In neither age was cell addition completely blocked, but more BrdU-ir cells were present in animals treated with AraC during puberty than during adulthood, perhaps reflecting the enhanced plasticity of the pubertal brain. One major consideration in the interpretation of the present results is that AraC treatment was not confined to just the AVPV. The origin of newly born cells in the AVPV is unknown, thus AraC was delivered ICV. However, ICV delivery of AraC via osmotic minipump is confined to ventricular regions, as BrdU-ir cells are observed within 2 hours of an ip BrdU injection in male and female rats (Mohr et al, in prep). Few, if any, BrdU-ir cells are observed in the amygdala of rats treated with ICV AraC and BrdU, whereas if BrdU is given ip to an animal receiving AraC and BrdU ICV there are BrdU-ir cells in the

amygdala (Figure 2.12), demonstrating the spread of AraC. It is possible that AraC treatment affected the addition of newly born cells to the arcuate nucleus of the hypothalamus, the home of estrogen negative feedback (for review see (Smith, 2013)). However, if this were the case, LH release in AraC treated animals might be tonic and not cyclical, and would be higher in AraC treated animals compared to age-matched controls. In an attempt to further implicate the role of pubertally and adult-born cells in the AVPV, specifically, in LH output, a regression analysis between BrdU-ir cells in the AVPV and mean maximum plasma LH concentration revealed a linear trend between the two variables. Thus, the more new cells that are added to the AVPV after puberty correlated in greater LH release from the pituitary, regardless of treatment (AraC vs. vehicle) or age during treatment (puberty vs. early adulthood). This underscores the role that newly born cells in the AVPV play in estrogen positive feedback.

Given the roles of IGF-1 in neuro- and gliogenesis in the preoptic area it is reasonable to speculate that IGF-1 stimulates the production of new cells in the AVPV, which are involved in the LH surge. Furthermore, decreased IGF-1 expression in adulthood could be the reason why fewer new cells are produced in the AVPV during adulthood. We have shown that decreased cell addition in the AVPV is correlated with lower LH output. In other words, IGF-1 could be stimulating the production of key cells that are involved in the regulation of GnRH release and consequently LH release. Decreased IGF-1 signaling with age could decrease the production of these key cells that regulate GnRH release. Indeed, constant infusion of IGF-1 receptor antagonist, JB-1 in 3-4 month Sprague-Dawley female rats attenuates both kisspeptin and NMDA-mediated LH release (Neal-Perry et al., 2014), similar to the effect AraC had on LH release. However, much more work is needed to determine a causal role between IGF-1 and

the stimulation of neurons and glia in the female rat AVPV that participate in estrogen positive feedback and the GnRH/LH surge.

While AraC treatment did not cause significant decreases in the proportion of newly born cells that express NeuN, AraC treatment during puberty increased the proportion of newly born cells that expressed GFAP, suggesting a compensation by newly born astrocytes when cell addition is knocked down during puberty. It is important to remember that even though the proportion of pubertally born astrocytes increased with AraC treatment, that the overall number of BrdU/GFAP colocalized cells was still much less in AraC-treated animals compared to control animals.

Even though AraC acts by specifically inhibiting mitosis, there have been reports that AraC can act as a cytotoxin (Sanz-Rodriguez et al., 1997). In the present study, if AraC were acting as a cytotoxin, the reduction in the LH surge could be because the underlying circuitry controlling estrogen positive feedback was damaged, and not because newborn cells are critically involved in the LH surge. To address any potential cytotoxic effects of centrally delivered AraC, Kokoeva and others elegantly demonstrated that AraC does not cause any cell degeneration throughout the brain parenchyma, using a sensitive marker of cell death, Fluoro-Jade, in AraC-treated mice (Kokoeva, 2005). These reports in mice alongside no observed changes in body weight or overall health of the AraC-treated rats in the present study suggest that AraC was not merely degrading the circuit underlying estrogen positive feedback, but that AraC was indeed acting as a mitotic inhibitor and newborn cells are involved in the full expression of an LH surge.

***Conclusion***

This study documents that cells are added to the AVPV during puberty and early adulthood and are functionally incorporated into neural circuits involved in estrogen positive feedback and generation of the GnRH/LH surge. These results imply that neuro- and gliogenesis in the female rat AVPV after puberty contribute to the maintenance of functional sexual dimorphisms.

**Table 1. Mean Plasma [LH] in Control vs. AraC-treated Rats**

| | Pubertal | | | Adult | | |
|---|---|---|---|---|---|---|
| **Time** | **Control (n = 4)** | **AraC (n=3)** | **Hedges' g** | **Control (n = 4)** | **AraC (n=4)** | **Hedges' g** |
| **1100** | 1.35 ± 0.31 | 1.22 ± 0.42 | 0.2* | 0.97 ± 0.16 | 0.8 ± 0 | 0.7** |
| **1200** | 14.83 ± 5.79 | 1.58 ± 0.44 | 1.2*** | 2.89 ± 1.30 | 1.43 ± 0.39 | 0.7** |
| **1300** | 35.90 ± 7.20 | 12.14 ± 4.10 | 1.6*** | 21.69 ± 11.15 | 9.03 ± 1.41 | 0.7** |
| **1350** | 46.29 ± 10.14 | 23.01 ± 4.97 | 1.1*** | 38.57 ± 11.59 | 14.06 ± 2.27 | 1.3*** |
| **1400** | 43.70 ± 9.09 | 29.36 ± 8.25 | 0.7** | 34.08 ± 8.95 | 16.22 ± 2.54 | 1.2*** |
| **1450** | 32.42 ± 6.05 | 27.85 ± 7.41 | 0.3* | 40.02 ± 12.09 | 15.99 ± 2.93 | 1.2*** |
| **1500** | 29.44 ± 7.62 | 25.91 ± 4.50 | 0.2* | 37.33 ± 10.09 | 16.02 ± 2.95 | 1.2*** |
| **1600** | 25.74 ± 5.71 | 20.19 ± 5.38 | 0.4* | 26.84 ± 7.83 | 12.29 ± 4.17 | 1.0*** |
| **1700** | 14.60 ± 4.07 | 14.12 ± 2.39 | 0.1 | 12.96 ± 1.34 | 9.54 ± 2.81 | 0.7** |
| **1800** | 5.32 ± 1.14 | 9.33 ± 3.34 | -0.8*** | 3.48 ± 0.58 | 4.59 ± 1.98 | -0.3** |
| **1900** | 2.47 ± 0.31 | 5.03 ± 1.35 | -1.3*** | 1.45 ± 0.23 | 1.83 ± 0.53 | -0.4** |

Means are expressed as mean plasma LH concentration ± SEM. * denotes a small effect size (>0.2), ** a medium effect (>0.5), and *** a large effect (>0.8)

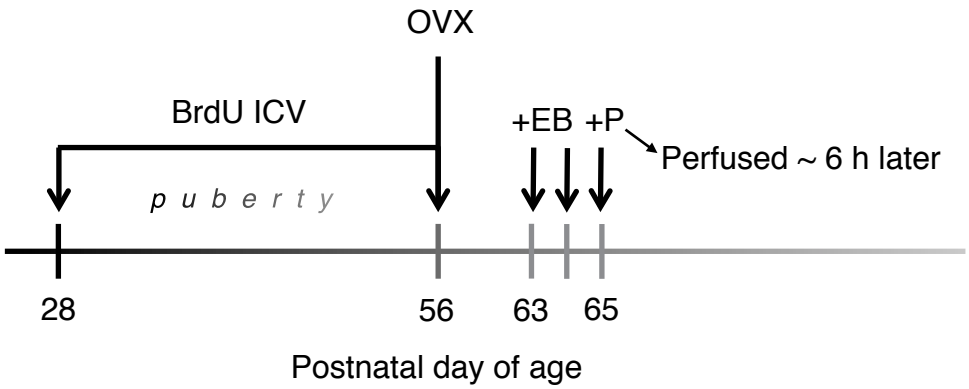


**Figure 2.1: Experimental timeline of experiment 2, to determine if cells born during puberty are active during the time of a hormone-induced LH surge.**

Female rats (n=16) received osmotic minipumps filled with BrdU (4.5 µg/µl in aCSF) on postnatal day (P) 28. At the end of ICV infusion (P56), animals were ovariectomized (OVX) and starting on P63, estradiol benzoate (EB; 10 µg in 0.05 ml sesame oil; subcutaneous) was given for two consecutive days at 1000 h. On P65, progesterone (P; 500 µg in 0.1 ml sesame oil; subcutaneous) was given at 1000h. Six hours after the P injection, all animals were perfused. Vehicle control animals received injections of just sesame oil for three days in a row.

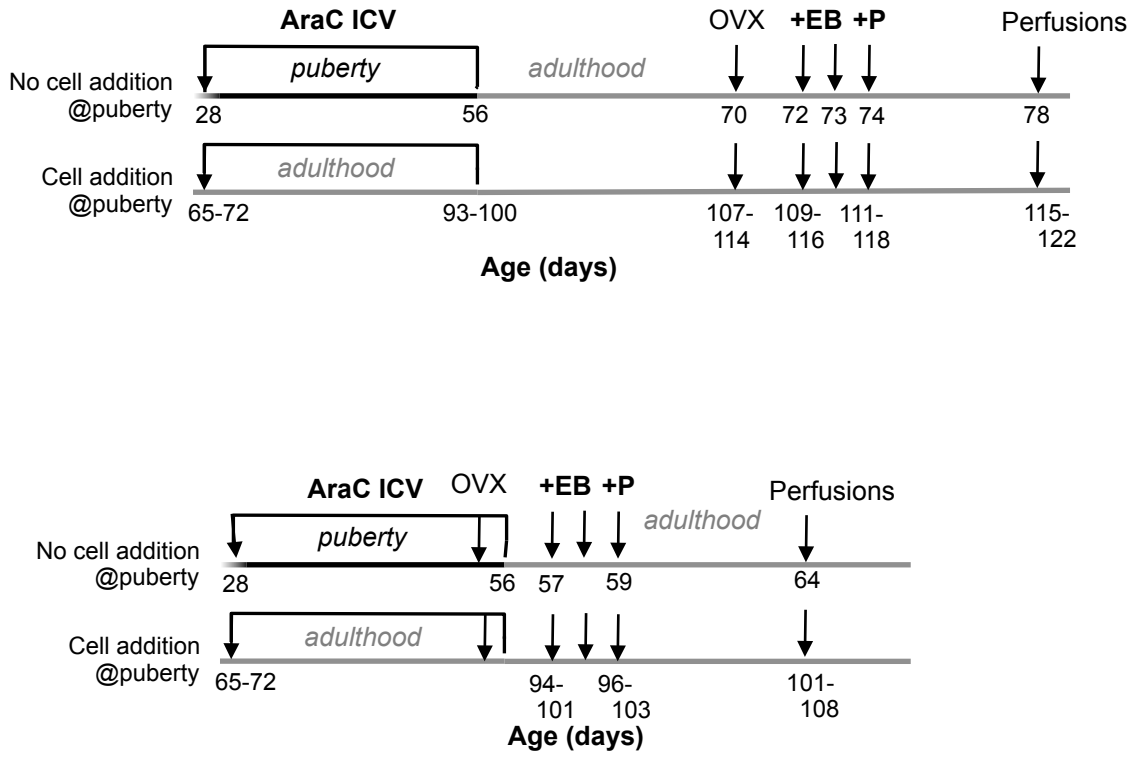


**Figure 2.2: Experimental timeline of experiment 3, to determine if inhibition of cell addition during or after puberty affects the ability to generate a hormone-induced LH surge.**

Female rats received osmotic minipumps filled with AraC (33 µg/µl in vehicle) with vehicle solution containing BrdU (4.5 µg/µl) in aCSF and infusion lasted for 4 weeks. Females were ovariectomized (OVX) at the end of ICV infusion or a couple weeks later, and then primed with estradiol benzoate (EB; 10 µg in 0.05 ml sesame oil; subcutaneous) for two consecutive days at 1000 h, and then progesterone (P; 500 µg in 0.1 ml sesame oil; subcutaneous) was given on the third day at 1000h. Blood sampling occurred on the same day as P injection, from 1100 h to 1900 h. A few days later, another LH surge was induced and the animals were perfused approximately 6 hours after P injection. Age-matched controls received just ICV vehicle infusion but otherwise were treated in the same manner as experimental animals.

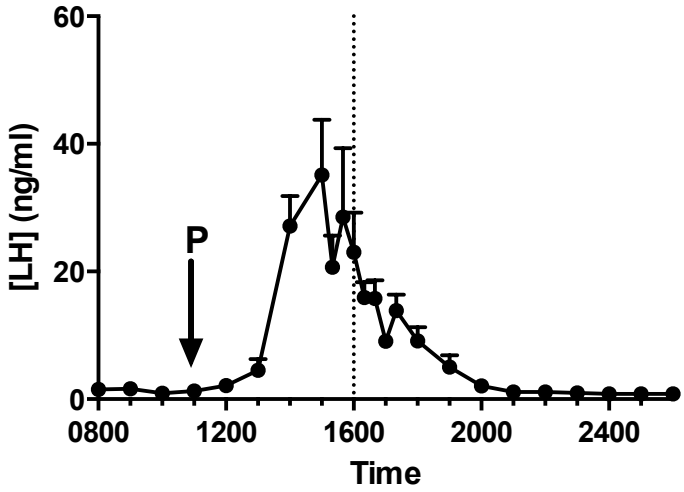


**Figure 2.3: Female rats show a surge of LH following priming with estradiol benzoate then progesterone.**

P injection took place at 1040 h (arrow). Vertical dotted line represents lights out. Data are presented as mean [LH] (ng/ml) ± SEM, n=3.

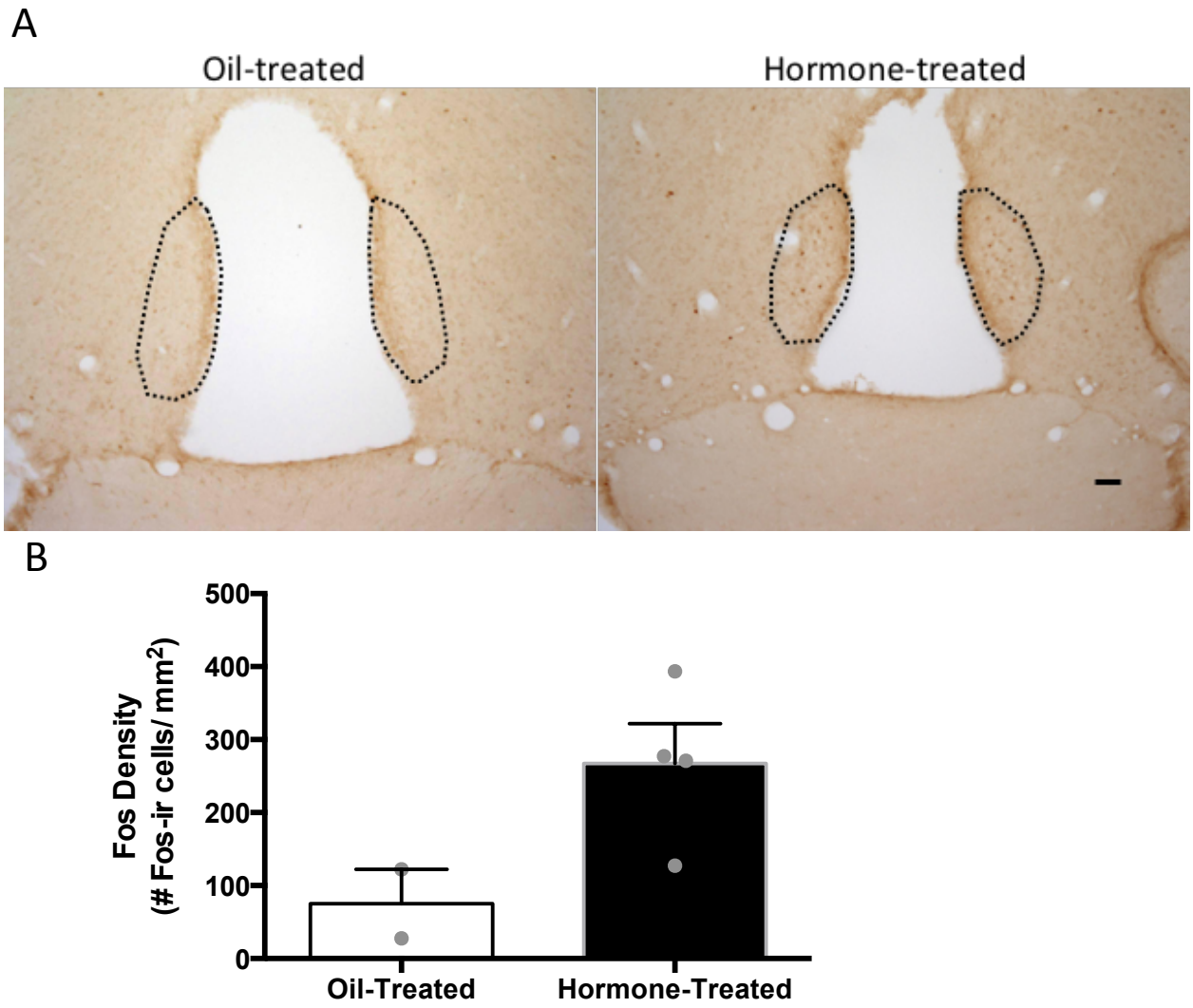


**Figure 2.4: Hormone-primed female rats show Fos-ir in the AVPV approximately 6 hours following P treatment.**

(A) Photomicrograph showing induction of Fos-ir in the AVPV after hormone priming, but not after oil treatment. Dotted lines show the location of the AVPV. Black scale bar indicates 50 µm. (B) Graph depicting Fos density (# Fos-ir cells/$mm^2$) in 4-5 sections of AVPV in oil- and hormone-treated ovariectomized female rats. Data are presented as means ± SEM, n=2 for oil-treated, n=4 for hormone-treated. Grey circles indicate individual data points.

A

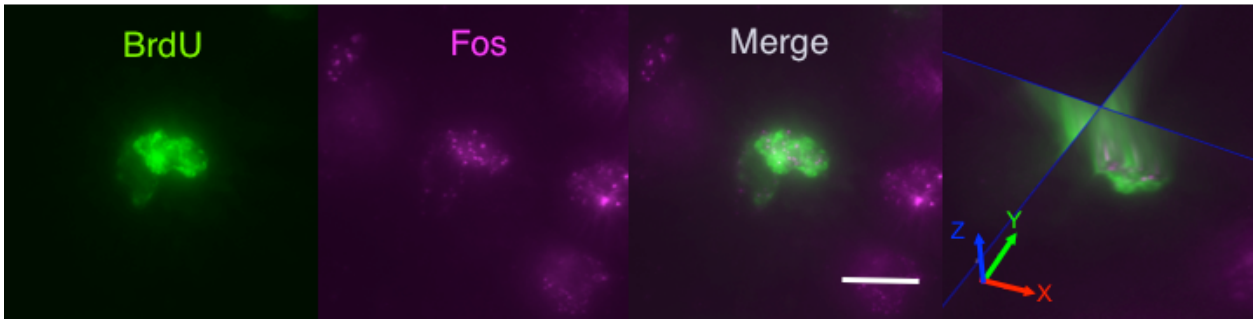


B

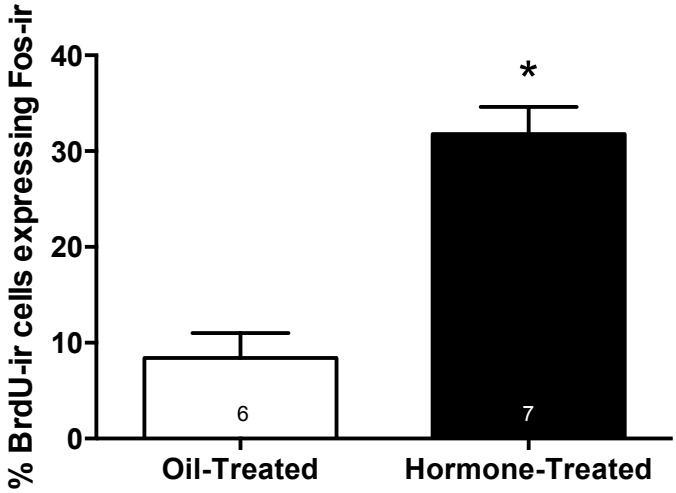


**Figure 2.5: Pubertally born cells are active at the time of the LH surge.**
(A) Representative photomicrograph of a pubertally born cell that is expressing Fos-ir after a hormone-induced LH surge. Images are a maximum intensity projection of a Z-stack (0.5 µm step) taken using MBF Bioscience's Image Stack Module. Scale bar indicates 10 µm. Orthogonal view through the middle of the cell confirms colocalization; the red arrow signifies the x plane, green arrow the y plane, and blue arrow the z plane. (B) Hormone-induction of the LH surge causes a significant increase in the percentage of BrdU-ir cells expressing Fos-ir during the time of the LH surge ($F(1,11) = 35.676$, $p \leq 0.0001$). Graph represents means ± SEMs, and numbers inside bars indicate n.

A

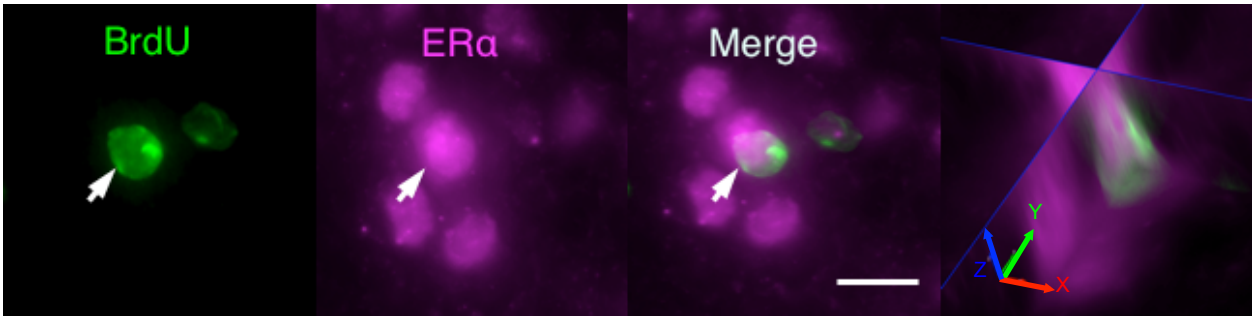


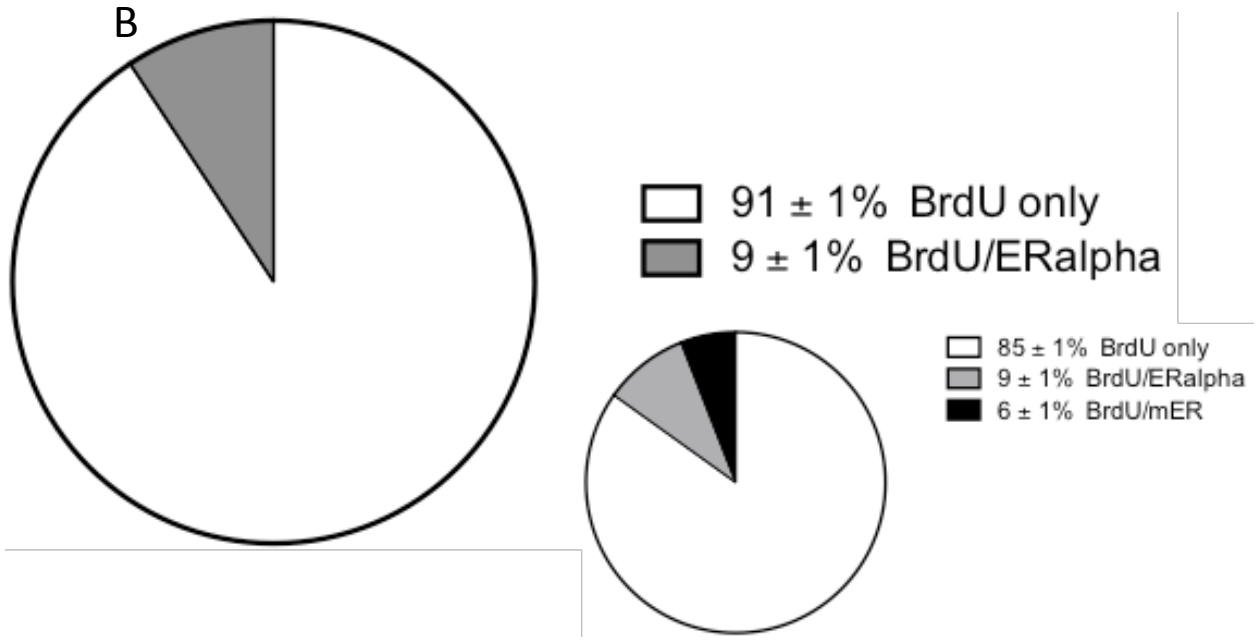


**Figure 2.6: Some pubertally born cells express ERα, but none express PR.**
(A) Z-stack images of a BrdU-ir cell colocalized with ERα-ir in the AVPV. BrdU, ERα, and Merge images are maximum intensity projections of 30 images (15 µm thick, 0.5 µm step). White scale bar represents 10 µm. Orthogonal view through the middle of the cell confirms colocalization; the red arrow signifies the x plane, green arrow the y plane, and blue arrow the z plane. (B) Pie chart depicting the mean percentage (± SEM) of BrdU-ir cells in the AVPV that colocalize with ERα.

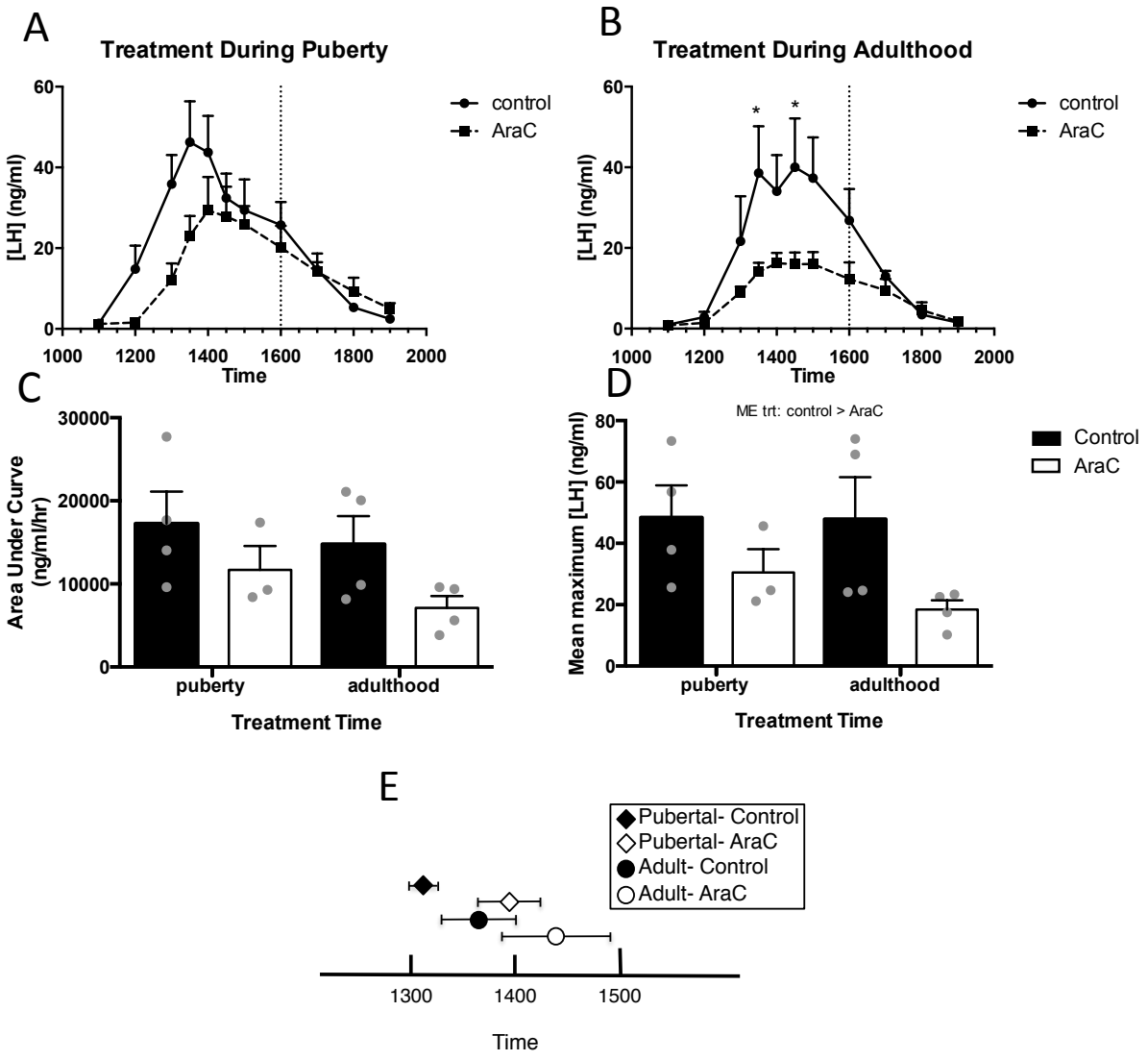


**Figure 2.7: Knockdown of cell addition during puberty or adulthood results in a delay and reduction of the LH surge.**

(A) AraC treatment during puberty and (B) during adulthood reduced the LH surge. Dotted vertical lines indicate lights off. (C) Area Under Curve calculations revealed that AraC treatment during puberty and during adulthood reduced the LH surge by 17% and 21%, respectively. (D) ANOVA revealed a main effect of treatment on mean maximum [LH], where AraC-treated animals had a lower maximum [LH] compared to control animals ($F(1,11) = 7.080$, $p = 0.022$). Grey circles indicate individual data points. (E) Mean timing of LH peak was delayed in AraC-treated animals ($F(1,11) = 4.412$, $p = 0.06$). Graphs represent means + SEMs, and n=4/grp, except for pubertal-AraC (n=3).

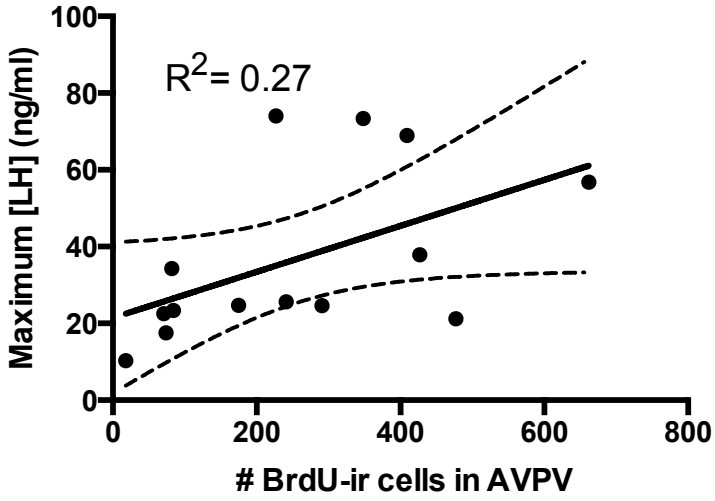


**Figure 2.8: Regardless of age or treatment, more cell addition in the AVPV is associated with higher concentration of LH in the blood following a hormone-induced LH surge.**
Individual maximum [LH] plotted against the number of BrdU-ir cells in 4 anatomically matched sections of the AVPV reveals a linear correlation between maximum [LH] observed after hormone priming and the number of pubertally and adult- born cells in the AVPV ($p$ = 0.058, $R^2$ = 0.27, slope = 0.06 ± 0.03). Solid line indicates slope, and dotted lines represent ± SEM.

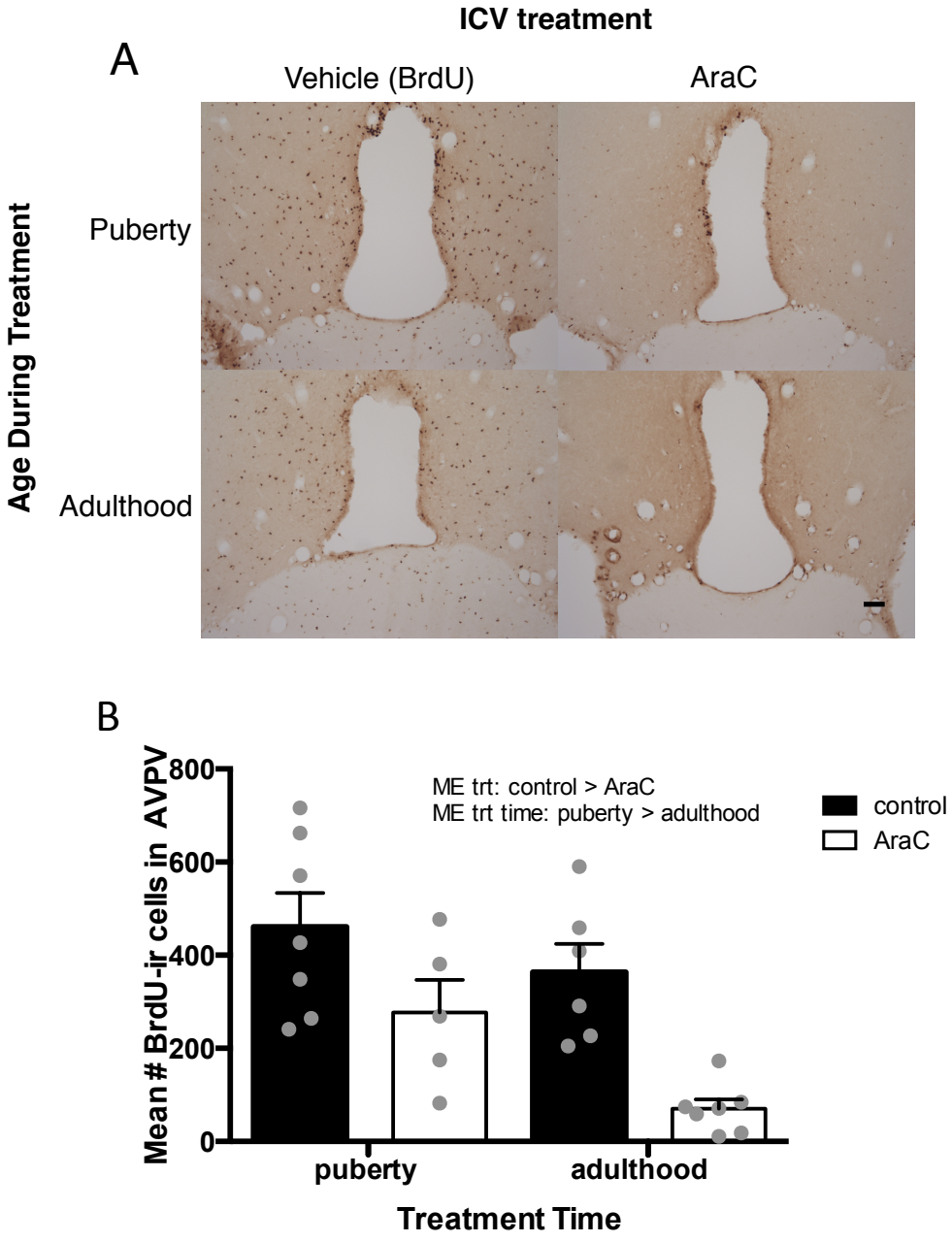


**Figure 2.9: ICV AraC treatment reduces the number of BrdU-ir cells in the AVPV and more cells are added to the AVPV during puberty than during adulthood.**

(A) Representative photomicrographs showing BrdU-ir cells in the AVPV of female rats treated with vehicle (BrdU in aCSF) or AraC during puberty or adulthood. Images taken at 100x magnification, black scale bar indicates 50 µm. (B) ANOVA revealed 2 significant main effects, with AraC-treated animals having less BrdU-ir cells than control animals that just got BrdU ($F(1,21) = 16.648$, $p \leq 0.001$), and there are more BrdU-ir cells in the AVPV of animals that were given BrdU during puberty compared to animals that were given BrdU during adulthood ($F(1,21) = 6.687$, $p = 0.017$). Graph represents means ± SEMs, and grey circles represent individual data points.

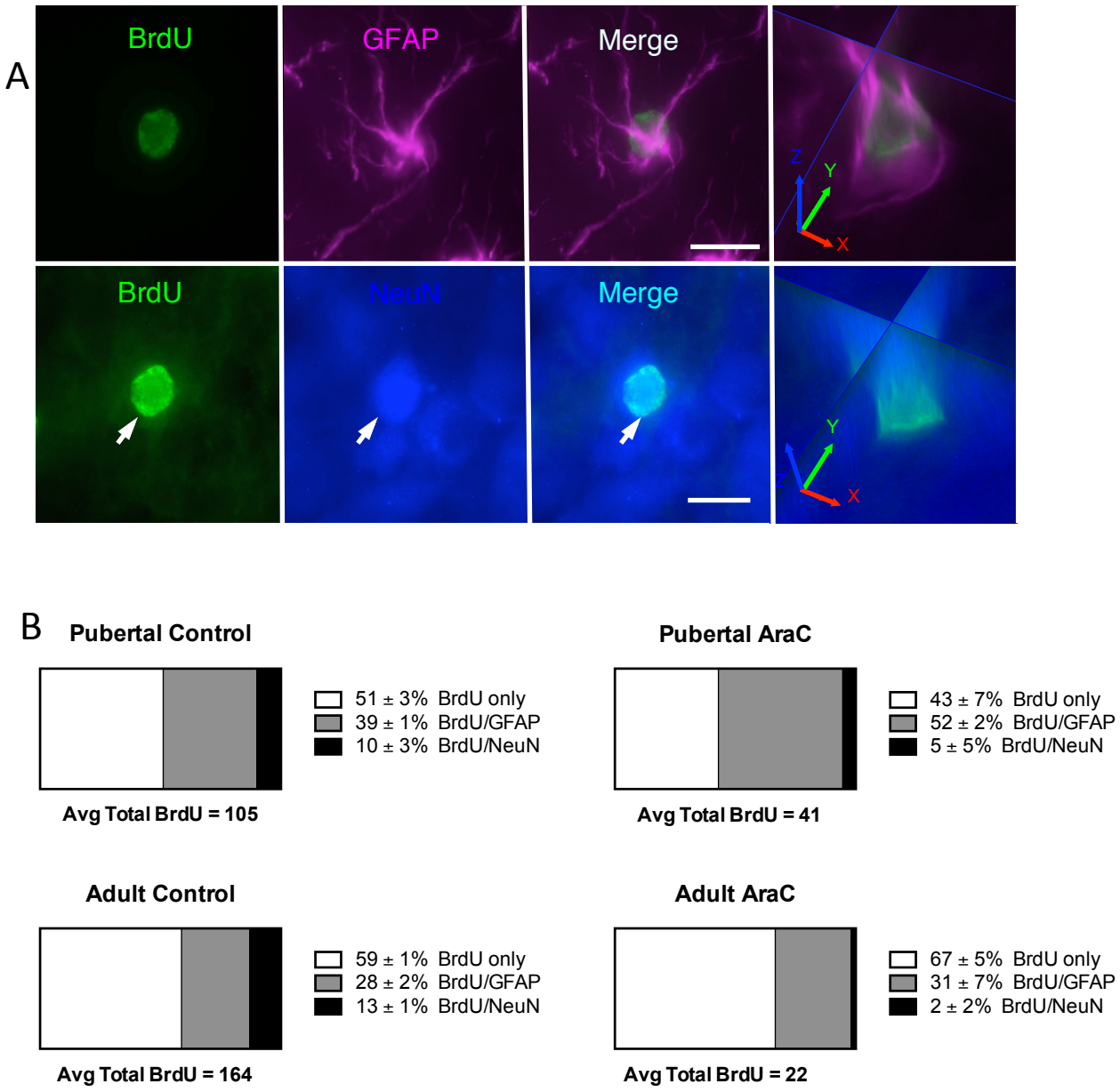


**Figure 2.10: Phenotypes of cells in the AVPV that were born during puberty or adulthood, with or without AraC-treatment.**

(A) Representative photomicrographs of pubertally born cells that expressing GFAP- or NeuN-ir. Images are a maximum intensity projection of a Z-stack (0.5 µm step) taken using MBF Bioscience's Image Stack Module. Scale bar indicates 10 µm. Orthogonal view through the middle of the cell confirms colocalization; the red arrow signifies the x plane, green arrow the y plane, and blue arrow the z plane. (B) Graphs represent the mean proportion of BrdU-ir cells that express neither label (BrdU only), or that also express GFAP-ir, or NeuN-ir (n=2/age/trt; means ± SEM).

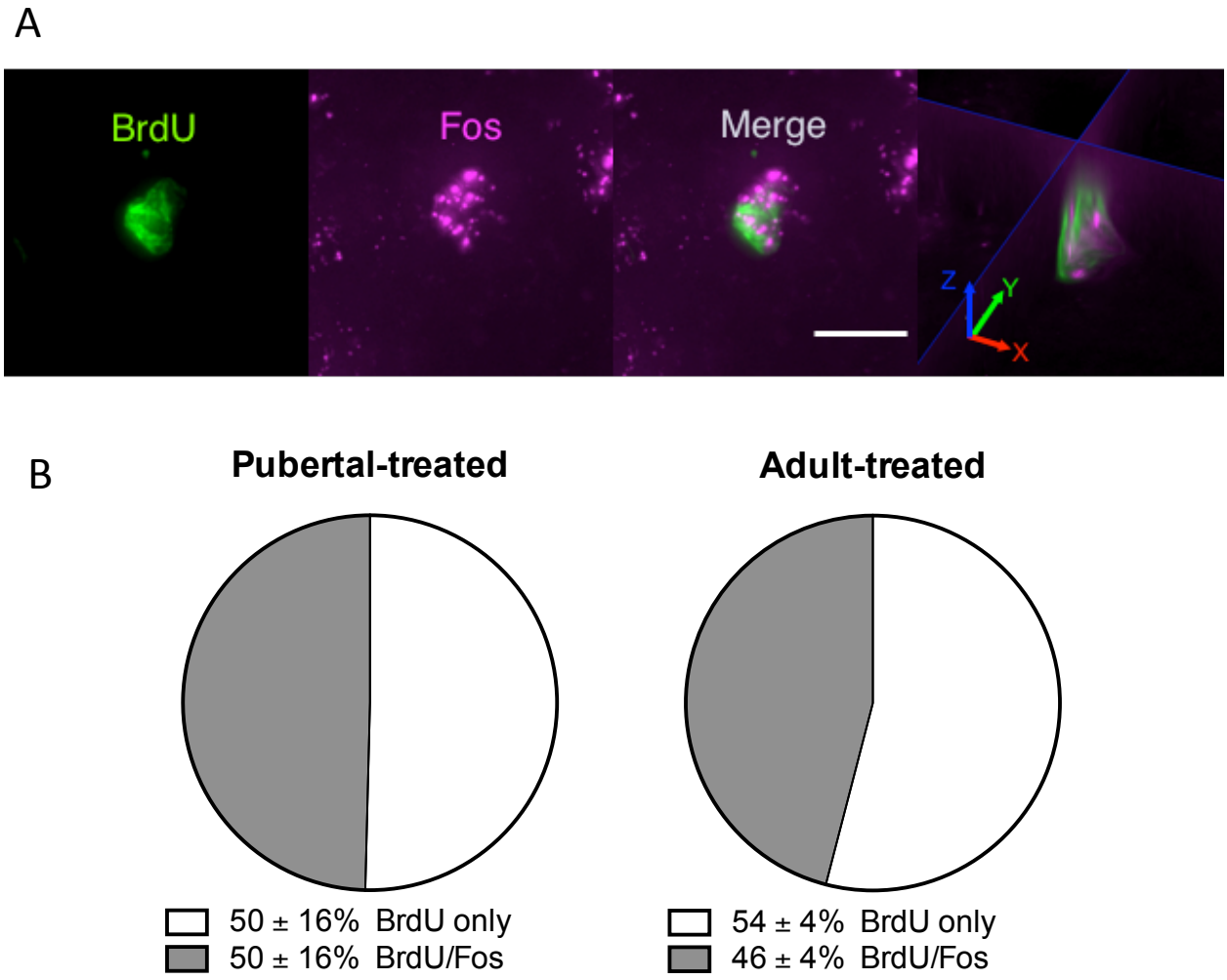


**Figure 2.11: Both pubertally born and adult born cells in the AVPV are active during a hormone-induced LH surge.**

(A) Z-stack images of a BrdU-ir cell colocalized with Fos-ir in the AVPV. BrdU, Fos, and Merge images are maximum intensity projections of 30 images (15 µm thick, 0.5 µm step). White scale bar represents 10 µm. Orthogonal view through the middle of the cell confirms colocalization; the red arrow signifies the x plane, green arrow the y plane, and blue arrow the z plane. (B) Pie charts depicting the percentage of pubertally or adult-born (BrdU-ir) cells in the AVPV that also express Fos-ir during the time of the LH surge in female rats that were treated with vehicle (BrdU in aCSF) during puberty or during adulthood. Data are presented as mean ± SEM, n=3/age.

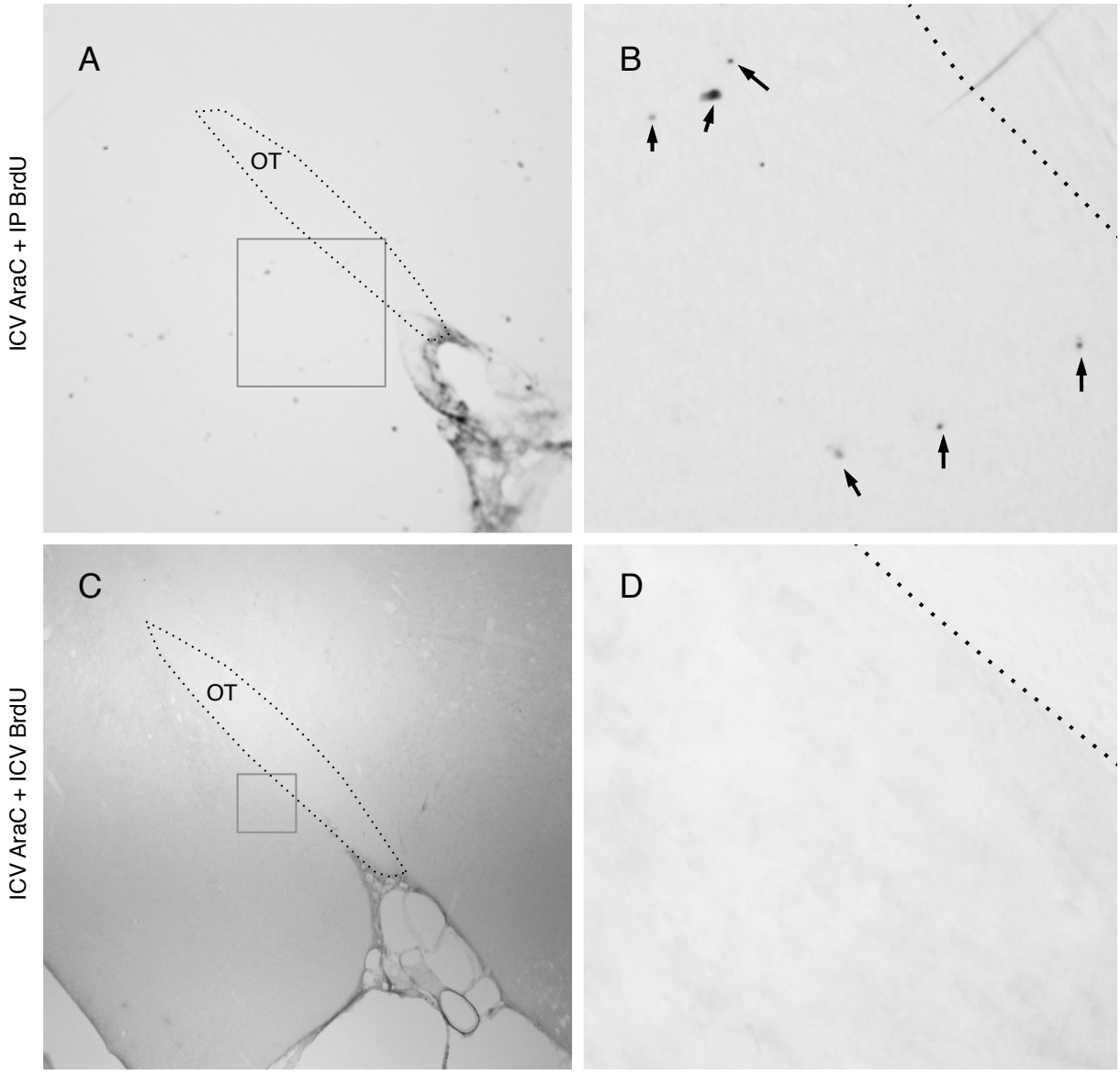


**Figure 2.12: Spread of ICV AraC/BrdU is confined to ventricular regions, and does not reach regions further in the parenchyma, such as the amygdala.**

Female rats treated with ICV AraC for 4 weeks and 5 days of ip BrdU injections display BrdU-ir cells in the amygdala (low power image in A, square indicates location of higher power image shown in B), whereas female rats treated with ICV AraC + BrdU have no BrdU-ir cells in the amygdala (low power image in C, square indicates location of higher power image shown in D). Dotted lines outline the optic tract (OT). Thus, AraC and BrdU delivered ICV are restricted to ventricular regions. Arrowheads point to BrdU-ir cells.

## CONCLUSION

For decades the dogma was that neurogenesis was confined to the initial construction of the nervous system during early development. Then, in the late 20th century came appreciation of adult neurogenesis and turnover of cells in the hippocampus and olfactory bulbs. Even more recently, there is growing evidence for adult neurogenesis that contributes to structural and functional plasticity in hypothalamic and limbic regions (Fowler et al., 2008; Kokoeva et al., 2005). Furthermore, disruptions in neurogenesis have been linked to mood disorders (Samuels and Hen, 2011) and to developmental disorders such as autism (Mercadante et al., 2008). Similarly, the first 50 years of research on the organization of sex differences in brain function mostly ignored the influence of hormones during puberty.

Neuroendocrinologists have believed for some time that although the HPG axis is awakened at puberty through some combination of removal of a brake and application of the gas pedal, the cellular machinery involved in the regulation of the HPG axis is in place long beforehand. These studies sought to challenge this theory by testing the hypothesis that pubertally added cells are critical for mature HPG axis function, and that the cellular machinery responsible for mature HPG axis regulation is *not* entirely in place before puberty. First, we wanted to confirm a female-biased sex difference that was previously seen in the addition of cells to the Sprague Dawley rat AVPV during early puberty, and to determine if this sex difference was due to greater cell addition in females, greater cell death in males, or a combination of the two possibilities. We found that cell addition in the rodent AVPV during puberty helps maintain morphological sex differences in this brain region, where more cells proliferate during early puberty in the female rat AVPV compared to the male, and the rate of

attrition is similar between the two sexes. We then demonstrated that the preoptic area of the brain is another neurogenic zone, where neurons, astrocytes, and microglia are born during puberty in the female rat. Next we demonstrated that pubertally born cells are functionally integrated into neural circuits that are involved in estrogen positive feedback and the generation of the GnRH/LH surge. Finally, we wanted to test whether cell addition, specifically during puberty, was a necessary for the launch of the LH surge. Much to our surprise, cell addition, including neuro- and gliogenesis, continues into adulthood in the female rat AVPV. Furthermore, pubertally and adult-born cells are active during the LH surge and knockdown of these cells decreases normal sex-specific HPG function, as measured by plasma LH output. The results of these studies shed light on cell addition as a contributing mechanism underlying sex-specific regulation of the HPG axis that emerges during puberty.

This research adds to a growing body of literature suggesting that the brain is extensively remodeled during puberty and adolescence. These studies provide a proof of principle that pubertal neuro- and gliogenesis are mechanisms of pubertal brain remodeling and hormonal regulation thereof. This has the potential to change the way we think about the development of behaviors and mature HPG axis function that occurs during this pivotal time point. There is a growing list of brain regions to which cells are added during puberty in rodents, including the AVPV, sexually dimorphic nucleus of the preoptic area (SDN-POA), medial amygdala (Ahmed et al., 2008), medial preoptic area (MPOA), arcuate nucleus (Mohr and Sisk, 2013), prefrontal cortex, nucleus accumbens (Staffend et al., 2014), the medial and lateral habenula (unpublished undergraduate project), and the basolateral amygdala (showing a male-biased sex difference in proliferation but not survival in rats; unpublished summer intern

project). When looking at tissue from a rodent that was given BrdU during puberty (be it a hamster, rat, or mouse), one might be surprised to see that BrdU-ir cells are just about everywhere in the brain. But, given the magnitude of the changes that occur to brain and behavior during puberty, an overhaul of circuits, *including the addition of cells to these circuits*, is not that far-fetched. Consideration of cell addition as a contributing mechanism to the pubertal remodeling of the brain will aid research investigating the development of maladaptive behaviors or disorders during puberty, and could even influence the administration of prescribed medication to teens that affects cell proliferation, such as antidepressants (Santarelli et al., 2003). Obviously, much more work is needed to determine the role that newborn cells are playing in the pubertal brain as it transitions into adulthood, but they could be contributing to behavioral flexibility, motivation, and/or part of hormonally sensitive circuits that control sex-specific functions.

The finding that cell addition continued into adulthood in the female rat AVPV was surprising. Based on the importance of the pubertal time period in organizing brain and behavior and the [seemingly false] notion that the adult brain is somewhat static in neuron number, except in the SVZ and SGZ, or in cases of injury, we originally hypothesized that knockdown of cell addition in adulthood would have no effect on the ability to generate an LH surge. We thought that cell addition during puberty, specifically, was key to this mature HPG axis function. So, when animals that were given AraC during adulthood had an even greater depreciation and delay of the LH surge, it changed the way we thought about cell addition in the AVPV. Not only are cells added to the AVPV during adulthood, albeit at lower levels compared to the amount added during puberty, but the adult-born cells are necessary for full

display of hypothalamic-pituitary responsiveness, and 50% of them are active during this hormonally mediated event! Newborn cells in the AVPV, whatever phenotype they may be, are abundantly involved in estrogen positive feedback and the GnRH/LH surge. The correlation between LH output and the number of newborn cells in the AVPV begs the question of whether or not decreased cell addition throughout adulthood contributes to reproductive senescence. Furthermore, if AraC had completely blocked cell addition to the AVPV, would an LH surge have occurred at all? If AraC were delivered directly into the third ventricle, would it have been more effective at inhibiting cell addition to the AVPV? The results of the current studies open the door to further examination into the maintenance of estrogen positive feedback in female rodents.

**REFERENCES**

REFERENCES


Ahern, T.H., et al., 2013. Cell death atlas of the postnatal mouse ventral forebrain and hypothalamus: effects of age and sex. J Comp Neurol. 521**,** 2551-69.

Ahmed, E.I., et al., 2008. Pubertal hormones modulate the addition of new cells to sexually dimorphic brain regions. Nature Neuroscience. 11**,** 995-997.

Anderson, M.F., et al., 2002. Insulin-like growth factor-I and neurogenesis in the adult mammalian brain. Brain Res Dev Brain Res. 134**,** 115-22.

Andrews, W.W., Mizejewski, G.J., Ojeda, S.R., 1981. Development of estradiol-positive feedback on luteinizing hormone release in the female rat: a quantitative study. Endocrinology. 109**,** 1404-13.

Bennett, M.R., Schwartz, W.J., 1994. Are glia among the cells that express immunoreactive c-Fos in the suprachiasmatic nucleus? Neuroreport. 5**,** 1737-40.

Bleier, R., Byne, W., Siggelkow, I., 1982. Cytoarchitectonic sexual dimorphisms of the medial preoptic and anterior hypothalamic areas in guinea pig, rat, hamster, and mouse. J Comp Neurol. 212**,** 118-30.

Bloch, G.J., Gorski, R.A., 1988. Estrogen/progesterone treatment in adulthood affects the size of several components of the medial preoptic area in the male rat. J Comp Neurol. 275**,** 613-22.

Bondar, G., et al., 2009. Estradiol-induced estrogen receptor-alpha trafficking. J Neurosci. 29**,** 15323-30.

Bouchard-Cannon, P., et al., 2013. The circadian molecular clock regulates adult hippocampal neurogenesis by controlling the timing of cell-cycle entry and exit. Cell Rep. 5**,** 961-73.

Caba, M., et al., 2003. Immunocytochemical detection of estrogen receptor-alpha in the female rabbit forebrain: topography and regulation by estradiol. Neuroendocrinology. 77**,** 208-22.

Cannon, J.R., Greenamyre, J.T., 2009. NeuN is not a reliable marker of dopamine neurons in rat substantia nigra. Neurosci Lett. 464**,** 14-7.

Cashion, A.B., Smith, M.J., Wise, P.M., 2003. The morphometry of astrocytes in the rostral preoptic area exhibits a diurnal rhythm on proestrus: relationship to the luteinizing hormone surge and effects of age. Endocrinology. 144**,** 274-80.

Chakraborty, T.R., et al., 2003. Stereologic analysis of estrogen receptor alpha (ER alpha) expression in rat hypothalamus and its regulation by aging and estrogen. J Comp Neurol. 466**,** 409-21.

Cheng, M.F., et al., 2011. Newborn GnRH neurons in the adult forebrain of the ring dove. Horm Behav. 60**,** 94-104.

Cheng, M.F., 2013. Hypothalamic neurogenesis in the adult brain. Front Neuroendocrinol. 34**,** 167-78.

Cifuentes, M., et al., 2011. A comparative analysis of intraperitoneal versus intracerebroventricular administration of bromodeoxyuridine for the study of cell proliferation in the adult rat brain. Journal of Neuroscience Methods. 201**,** 307-314.

Clarkson, J., et al., 2008. Kisspeptin-GPR54 signaling is essential for preovulatory gonadotropin-releasing hormone neuron activation and the luteinizing hormone surge. J Neurosci. 28**,** 8691-7.

Daftary, S.S., Gore, A.C., 2005. IGF-1 in the brain as a regulator of reproductive neuroendocrine function. Exp Biol Med (Maywood). 230**,** 292-306.

Davis, E.C., Shryne, J.E., Gorski, R.A., 1996. Structural sexual dimorphisms in the anteroventral periventricular nucleus of the rat hypothalamus are sensitive to gonadal steroids perinatally, but develop peripubertally. Neuroendocrinology. 63**,** 142-8.

Dhandapani, K.M., Mahesh, V.B., Brann, D.W., 2003. Astrocytes and brain function: implications for reproduction. Exp Biol Med (Maywood). 228**,** 253-60.

Forger, N.G., et al., 2004. Deletion of Bax eliminates sex differences in the mouse forebrain. Proc Natl Acad Sci U S A. 101**,** 13666-71.

Fowler, C.D., Freeman, M.E., Wang, Z., 2003. Newly proliferated cells in the adult male amygdala are affected by gonadal steroid hormones. J Neurobiol. 57**,** 257-69.

Fowler, C.D., Johnson, F., Wang, Z., 2005. Estrogen regulation of cell proliferation and distribution of estrogen receptor-$\alpha$ in the brains of adult female prairie and meadow voles. J Comp Neurol. 489**,** 166-179.

Fowler, C.D., Liu, Y., Wang, Z., 2008. Estrogen and adult neurogenesis in the amygdala and hypothalamus. Brain Res Rev. 57**,** 342-51.

Garcia-Segura, L.M., Lorenz, B., DonCarlos, L.L., 2008. The role of glia in the hypothalamus: implications for gonadal steroid feedback and reproductive neuroendocrine output. Reproduction. 135**,** 419-429.

Glanowska, K.M., Burger, L.L., Moenter, S.M., 2014. Development of gonadotropin-releasing hormone secretion and pituitary response. J Neurosci. 34**,** 15060-9.

Goodman, R.L., 1978. The site of the positive feedback action of estradiol in the rat. Endocrinology. 102**,** 151-9.

Gore, A.C., Roberts, J.L., Gibson, M.J., 1999. Mechanisms for the regulation of gonadotropin-releasing hormone gene expression in the developing mouse. Endocrinology. 140**,** 2280-7.

He, J., Crews, F.T., 2007. Neurogenesis decreases during brain maturation from adolescence to adulthood. Pharmacol Biochem Behav. 86**,** 327-33.

Hengerer, B., et al., 1990. Lesion-induced increase in nerve growth factor mRNA is mediated by c-fos. Proc Natl Acad Sci U S A. 87**,** 3899-903.

Hisanaga, K., et al., 1990. c-fos proto-oncogene expression in astrocytes associated with differentiation or proliferation but not depolarization. Brain Res Mol Brain Res. 8**,** 69-75.

Hoffman, G.E., et al., 1990. Luteinizing hormone-releasing hormone neurons express c-fos antigen after steroid activation. Endocrinology. 126**,** 1736-41.

Hoffman, G.E., et al., 1993. c-Fos and Fos-related antigens as markers for neuronal activity: perspectives from neuroendocrine systems. NIDA Res Monogr. 125**,** 117-33.

Hoffman, G.E., et al., 2005. Estrogen and progesterone do not activate Fos in AVPV or LHRH neurons in male rats. Brain Res. 1054**,** 116-24.

Ito, S., et al., 1986. Prenatal androgen exposure, preoptic area and reproductive functions in the female rat. Brain Dev. 8**,** 463-8.

Kalra, P.S., McCann, S.M., 1975. The stimulatory effect on gonadotropin release of implants of estradiol or progesterone in certain sites in the central nervous system. Neuroendocrinology. 19**,** 289-302.

Kauffman, A.S., 2010. Gonadal and nongonadal regulation of sex differences in hypothalamic Kiss1 neurones. J Neuroendocrinol. 22**,** 682-91.

Kauffman, A.S., Smith, J.T., 2013. Kisspeptin Signaling in Reproductive Biology Preface. In: Kisspeptin Signaling in Reproductive Biology. Advances in Experimental Medicine and Biology, Vol. 784, A.S. Kauffman, J.T. Smith, ed.^eds., pp. V-VI.

Kokoeva, M.V., 2005. Neurogenesis in the Hypothalamus of Adult Mice: Potential Role in Energy Balance. Science. 310**,** 679-683.

Kokoeva, M.V., Yin, H., Flier, J.S., 2005. Neurogenesis in the hypothalamus of adult mice: potential role in energy balance. Science. 310**,** 679-83.

Kokoeva, M.V., Yin, H., Flier, J.S., 2007. Evidence for constitutive neural cell proliferation in the adult murine hypothalamus. J Comp Neurol. 505**,** 209-20.

Kuo, J., et al., 2010a. Sex differences in hypothalamic astrocyte response to estradiol stimulation. Biol Sex Differ. 1**,** 7.

Kuo, J., et al., 2010c. Membrane estrogen receptors stimulate intracellular calcium release and progesterone synthesis in hypothalamic astrocytes. J Neurosci. 30**,** 12950-7.

Kuo, J., Micevych, P., 2012. Neurosteroids, trigger of the LH surge. J Steroid Biochem Mol Biol. 131**,** 57-65.

Ladenheim, R.G., et al., 1993. Endothelins stimulate c-fos and nerve growth factor expression in astrocytes and astrocytoma. J Neurochem. 60**,** 260-6.

Lau, B.W.-M., et al., 2011. Effect of Corticosterone and Paroxetine on Masculine Mating Behavior: Possible Involvement of Neurogenesis. The Journal of Sexual Medicine. 8**,** 1390-1403.

Lee, D.A., et al., 2012. Tanycytes of the hypothalamic median eminence form a diet-responsive neurogenic niche. Nat Neurosci. 15**,** 700-2.

Lee, W.S., Smith, M.S., Hoffman, G.E., 1990. Luteinizing hormone-releasing hormone neurons express Fos protein during the proestrous surge of luteinizing hormone. Proc Natl Acad Sci U S A. 87**,** 5163-7.

Lenz, K.M., et al., 2013. Microglia are essential to masculinization of brain and behavior. J Neurosci. 33**,** 2761-72.

Lenz, K.M., McCarthy, M.M., 2015. A starring role for microglia in brain sex differences. Neuroscientist. 21**,** 306-21.

Llorens-Martin, M., Torres-Aleman, I., Trejo, J.L., 2009. Mechanisms mediating brain plasticity: IGF1 and adult hippocampal neurogenesis. Neuroscientist. 15**,** 134-48.

Matsunaga, W., et al., 2001. Astrocytic Fos expression in the rat posterior pituitary following LPS administration. Brain Res. 898**,** 215-23.

Mayer, C., et al., 2010. Timing and completion of puberty in female mice depend on estrogen receptor  -signaling in kisspeptin neurons. Proceedings of the National Academy of Sciences. 107**,** 22693-22698.

Mercadante, M.T., et al., 2008. Neurogenesis in the amygdala: a new etiologic hypothesis of autism? Med Hypotheses. 70**,** 352-7.

Micevych, P., et al., 2003a. The luteinizing hormone surge is preceded by an estrogen-induced increase of hypothalamic progesterone in ovariectomized and adrenalectomized rats. Neuroendocrinology. 78**,** 29-35.

Micevych, P., et al., 2003c. The Luteinizing Hormone Surge Is Preceded by an Estrogen-Induced Increase of Hypothalamic Progesterone in Ovariectomized and Adrenalectomized Rats. Neuroendocrinology. 78**,** 29-35.

Micevych, P., Sinchak, K., 2011. The Neurosteroid Progesterone Underlies Estrogen Positive Feedback of the LH Surge. Front Endocrinol (Lausanne). 2**,** 90.

Micevych, P.E., et al., 2007. Estradiol stimulates progesterone synthesis in hypothalamic astrocyte cultures. Endocrinology. 148**,** 782-9.

Migaud, M., et al., 2010. Emerging new sites for adult neurogenesis in the mammalian brain: a comparative study between the hypothalamus and the classical neurogenic zones. Eur J Neurosci. 32**,** 2042-52.

Miller, B.H., Gore, A.C., 2001. Alterations in hypothalamic insulin-like growth factor-I and its associations with gonadotropin releasing hormone neurones during reproductive development and ageing. J Neuroendocrinol. 13**,** 728-36.

Mohr, M.A., Sisk, C.L., 2013. Pubertally born neurons and glia are functionally integrated into limbic and hypothalamic circuits of the male Syrian hamster. Proc Natl Acad Sci U S A. 110**,** 4792-7.

Morin, L.P., Hefton, S., Studholme, K.M., 2011. Neurons identified by NeuN/Fox-3 immunoreactivity have a novel distribution in the hamster and mouse suprachiasmatic nucleus. Brain Res. 1421**,** 44-51.

Mullen, R.J., Buck, C.R., Smith, A.M., 1992. NeuN, a neuronal specific nuclear protein in vertebrates. Development. 116**,** 201-11.

Neal-Perry, G., et al., 2014. Insulin-like growth factor-I regulates LH release by modulation of kisspeptin and NMDA-mediated neurotransmission in young and middle-aged female rats. Endocrinology. 155**,** 1827-37.

Nimmerjahn, A., Kirchhoff, F., Helmchen, F., 2005. Resting microglial cells are highly dynamic surveillants of brain parenchyma in vivo. Science. 308**,** 1314-8.

Nishizuka, M., et al., 1993. Formation of neurons in the sexually dimorphic anteroventral periventricular nucleus of the preoptic area of the rat: effects of prenatal treatment with testosterone propionate. J Neuroendocrinol. 5**,** 569-73.

Ojeda, S.R., Lomniczi, A., Sandau, U., 2010. Contribution of glial-neuronal interactions to the neuroendocrine control of female puberty. Eur J Neurosci. 32**,** 2003-10.

Ojeda SR, U.H., 1994. Puberty in the Rat. In: Knobil E, Neill JD, eds. The physiology of reproduction. Vol. 2nd ed. Vol 2, ed.^eds. Raven Press, New York, pp. 363-409.

Okamoto, M., et al., 2012. Mild exercise increases dihydrotestosterone in hippocampus providing evidence for androgenic mediation of neurogenesis. Proc Natl Acad Sci U S A. 109**,** 13100-5.

Overgaard, A., et al., 2013. Comparative analysis of kisspeptin-immunoreactivity reveals genuine differences in the hypothalamic Kiss1 systems between rats and mice. Peptides. 45**,** 85-90.

Pawluski, J.L., et al., 2009. Effects of steroid hormones on neurogenesis in the hippocampus of the adult female rodent during the estrous cycle, pregnancy, lactation and aging. Front Neuroendocrinol. 30**,** 343-57.

Perez-Martin, M., et al., 2010. IGF-I stimulates neurogenesis in the hypothalamus of adult rats. Eur J Neurosci. 31**,** 1533-48.

Petersen, S.L., Barraclough, C.A., 1989. Suppression of spontaneous LH surges in estrogen-treated ovariectomized rats by microimplants of antiestrogens into the preoptic brain. Brain Res. 484**,** 279-89.

Petersen, S.L., et al., 1989. Medial preoptic microimplants of the antiestrogen, keoxifene, affect luteinizing hormone-releasing hormone mRNA levels, median eminence luteinizing hormone-releasing hormone concentrations and luteinizing hormone release in ovariectomized, estrogen-treated rats. J Neuroendocrinol. 1**,** 279-83.

Pierce, A.A., Xu, A.W., 2010. De novo neurogenesis in adult hypothalamus as a compensatory mechanism to regulate energy balance. J Neurosci. 30**,** 723-30.

Portiansky, E.L., et al., 2006. Loss of NeuN immunoreactivity in rat spinal cord neurons during aging. Exp Neurol. 202**,** 519-21.

Rojczyk-Golebiewska, E., Palasz, A., Wiaderkiewicz, R., 2014. Hypothalamic subependymal niche: a novel site of the adult neurogenesis. Cell Mol Neurobiol. 34**,** 631-42.

Samuels, B.A., Hen, R., 2011. Neurogenesis and affective disorders. Eur J Neurosci. 33**,** 1152-9.

Santarelli, L., et al., 2003. Requirement of hippocampal neurogenesis for the behavioral effects of antidepressants. Science. 301**,** 805-9.

Sanz-Rodriguez, C., Boix, J., Comella, J.X., 1997. Cytosine arabinoside is neurotoxic to chick embryo spinal cord motoneurons in culture. Neurosci Lett. 223**,** 141-4.

Simerly, R.B., Swanson, L.W., Gorski, R.A., 1985. The distribution of monoaminergic cells and fibers in a periventricular preoptic nucleus involved in the control of gonadotropin release: immunohistochemical evidence for a dopaminergic sexual dimorphism. Brain Res. 330**,** 55-64.

Simerly, R.B., et al., 1996. Ovarian steroid regulation of estrogen and progesterone receptor messenger ribonucleic acid in the anteroventral periventricular nucleus of the rat. J Neuroendocrinol. 8**,** 45-56.

Simerly, R.B., 2002. Wired for reproduction: organization and development of sexually dimorphic circuits in the mammalian forebrain. Annu Rev Neurosci. 25**,** 507-36.

Sinchak, K., et al., 2003. Estrogen Induces de novo Progesterone Synthesis in Astrocytes. Developmental Neuroscience. 25**,** 343-348.

Sisk, C.L., Desjardins, C., 1986. Pulsatile release of luteinizing hormone and testosterone in male ferrets. Endocrinology. 119**,** 1195-203.

Sisk, C.L., et al., 2001. In vivo gonadotropin-releasing hormone secretion in female rats during peripubertal development and on proestrus. Endocrinology. 142**,** 2929-36.

Smarr, B.L., Gile, J.J., de la Iglesia, H.O., 2013. Oestrogen-independent circadian clock gene expression in the anteroventral periventricular nucleus in female rats: possible role as an integrator for circadian and ovarian signals timing the luteinising hormone surge. J Neuroendocrinol. 25**,** 1273-9.

Smith, J.T., 2013. Sex steroid regulation of kisspeptin circuits. Adv Exp Med Biol. 784**,** 275-95.

Snyder, J.S., et al., 2009. Adult-born hippocampal neurons are more numerous, faster maturing, and more involved in behavior in rats than in mice. J Neurosci. 29**,** 14484-95.

Snyder, J.S., Ferrante, S.C., Cameron, H.A., 2012. Late maturation of adult-born neurons in the temporal dentate gyrus. PLoS One. 7**,** e48757.

Staffend, N.A., et al., 2014. A decrease in the addition of new cells in the nucleus accumbens and prefrontal cortex between puberty and adulthood in male rats. Dev Neurobiol. 74**,** 633-42.

Sumida, H., et al., 1993. Sex differences in the anteroventral periventricular nucleus of the preoptic area and in the related effects of androgen in prenatal rats. Neurosci Lett. 151**,** 41-4.

Tanapat, P., et al., 1999. Estrogen stimulates a transient increase in the number of new neurons in the dentate gyrus of the adult female rat. J Neurosci. 19**,** 5792-801.

Tanapat, P., Hastings, N.B., Gould, E., 2005. Ovarian steroids influence cell proliferation in the dentate gyrus of the adult female rat in a dose- and time-dependent manner. J Comp Neurol. 481**,** 252-65.

Tchelingerian, J.L., et al., 1997. Widespread neuronal expression of c-Fos throughout the brain and local expression in glia following a hippocampal injury. Neurosci Lett. 226**,** 175-8.

Ullian, E.M., et al., 2001. Control of synapse number by glia. Science. 291**,** 657-61.

Unal-Cevik, I., et al., 2004. Loss of NeuN immunoreactivity after cerebral ischemia does not indicate neuronal cell loss: a cautionary note. Brain Res. 1015**,** 169-74.

Vazquez-Villoldo, N., et al., 2014. P2X4 receptors control the fate and survival of activated microglia. Glia. 62**,** 171-84.

Waters, E.M., Simerly, R.B., 2009. Estrogen Induces Caspase-Dependent Cell Death during Hypothalamic Development. Journal of Neuroscience. 29**,** 9714-9718.

Wiegand, S.J., et al., 1980. Effects of discrete lesions of preoptic and suprachiasmatic structures in the female rat. Alterations in the feedback regulation of gonadotropin secretion. Neuroendocrinology. 31**,** 147-57.

Wiegand, S.J., Terasawa, E., 1982. Discrete lesions reveal functional heterogeneity of suprachiasmatic structures in regulation of gonadotropin secretion in the female rat. Neuroendocrinology. 34**,** 395-404.

Wintermantel, T.M., et al., 2006. Definition of estrogen receptor pathway critical for estrogen positive feedback to gonadotropin-releasing hormone neurons and fertility. Neuron. 52**,** 271-80.

Xu, Y., et al., 2005. Neurogenesis in the ependymal layer of the adult rat 3rd ventricle. Exp Neurol. 192**,** 251-64.

Yuan, H., et al., 2010. Acute hyperosmotic stimulus-induced Fos expression in neurons depends on activation of astrocytes in the supraoptic nucleus of rats. Journal of Neuroscience Research. 88**,** 1364-1373.

Zup, S.L., et al., 2003. Overexpression of bcl-2 reduces sex differences in neuron number in the brain and spinal cord. J Neurosci. 23**,** 2357-62.